

## Strongly correlated electronic systems with one hole: Dynamical properties

Elbio Dagotto, Robert Joynt, and Adriana Moreo

*Institute of Theoretical Physics and Physics Department, University of California at Santa Barbara, Santa Barbara, California 93106*

Silvia Bacci and Eduardo Gagliano

*Physics Department and Material Research Laboratory, University of Illinois at Urbana-Champaign, Urbana, Illinois 61801*

(Received 5 December 1989)

The spectral functions of one hole in the  $t$ - $J$  and one-band Hubbard models are calculated using exact diagonalization techniques on small lattices. Results for the  $t$ - $J_z$  model are also presented. For the  $t$ - $J$  model we found that there is a quasiparticle at the bottom of the hole spectrum with an energy well approximated by  $E_h = -3.17 + 2.83J^{0.73}$  (for  $0.1 \leq J \leq 1.0$ ,  $t = 1$ ) on a  $4 \times 4$  lattice. The rest of the spectrum is not incoherent: We identified at least two other peaks following a similar power-law behavior with  $J$ . We speculate that the  $J$  dependence of the results can be explained by a model where the hole is trapped in a confining potential as in the Ising limit. The bandwidth of the hole is linear in  $J$  in the region  $0.1 \leq J \leq 0.4$  although a power-law behavior is not excluded. The spectral weight of the quasiparticle grows like  $J^{0.5}$  in the same region. We present new analytical results in the large  $J/t$  limit to understand the motion of the hole: In perturbation theory it can be shown that the momentum of the hole at large  $J/t$  is  $\mathbf{k} = (\pi, \pi)$  changing to  $\mathbf{k} = (\pi/2, \pi/2)$  at intermediate  $J/t$  in agreement with numerical and spin-waves results. We show analytically and numerically that the bandwidth of the quasiparticle is of order  $t$  in the large  $J/t$  limit. This result corresponds to a spin-liquid state. The one-hole spectral function of the Hubbard model is obtained for lattices with 8 and 10 sites. A quasiparticle is also observed in this case. The bandwidth and the relation with the  $t$ - $J$  model are discussed and a comparison with recent Monte Carlo results is made. We also review and extend previous results for the ground-state properties of the  $t$ - $J$  model.

### I. INTRODUCTION

The discovery of high-temperature superconductors<sup>1</sup> has induced considerable theoretical work on strongly correlated electronic systems in two dimensions. Most of the effort has been concentrated on the one- and two-band Hubbard models where electrons interact through an on-site Coulombic repulsion. Experimental results suggest that this model should be analyzed in the strong coupling region ( $U/t \gg 1$  in the standard notation). In that limit the problem can be further simplified<sup>2</sup> by replacing the Hubbard model by the  $t$ - $J$  model defined by the Hamiltonian

$$H = J \sum_{i, \delta} \mathbf{S}_i \cdot \mathbf{S}_{i+\delta} - t \sum_{i, \delta, \sigma} (\bar{c}_{i, \sigma}^\dagger \bar{c}_{i+\delta, \sigma} + \text{H.c.}), \quad (1)$$

where the first term represents the antiferromagnetic Heisenberg interaction between two nearest-neighbors electrons while the hopping term allows holes to move.  $\hat{\delta}$  denotes unit vectors in both directions of a square lattice while  $i$  denotes the sites of that lattice.  $\{c_{i, \sigma}\}$  are standard fermionic operators on site  $i$  with spin index ( $\sigma = \uparrow, \downarrow$ ) while  $\bar{c}_{i, \sigma}^\dagger$  is a hole operator defined as  $\bar{c}_{i, \sigma}^\dagger = c_{i, \sigma} (1 - n_{i, -\sigma})$ , where  $n_{i, -\sigma} = c_{i, -\sigma}^\dagger c_{i, -\sigma}$  is the number operator. The spin operator  $\mathbf{S}_i$  is defined as

$$\mathbf{S}_i = \frac{1}{2} \sum_{\alpha, \beta} c_{i, \alpha}^\dagger \boldsymbol{\sigma}_{\alpha, \beta} c_{i, \beta}, \quad (2)$$

where  $\alpha, \beta = \uparrow, \downarrow$ . The parameters of the one-band Hubbard and  $t$ - $J$  models are related through  $J = 4t^2/U$ .

Many studies have been presented in the literature about the static ground-state properties of the  $t$ - $J$  model in different regimes. Those results will be reviewed and extended in Sec. II. One of the main purposes of this paper is to present numerical and analytical results for the dynamics of this model, a subject somewhat controversial and not much explored. The one-dimensional case has been studied using spin-wave techniques.<sup>3</sup> Recently, a self-consistent diagrammatic calculation for the  $t$ - $J$  model in two dimensions has been presented,<sup>4</sup> where an infinite subset of Feynman diagrams was summed. In that paper it was found that the hole spectral function presents a quasiparticle peak at finite  $J/t$  while at  $J/t = 0$  we know<sup>5</sup> that the band is incoherent. The hole acquires a large effective mass and the bandwidth is of order  $J$ . The reason is that in the  $t$ - $J$  model the hole hops from even to odd sites distorting the Néel structure of the background. That costs energy which induces the large effective mass of the hole. These important predictions need confirmation based on numerical techniques since the approximations used in their derivation are not well under control. However, a numerical study is also difficult since Monte Carlo techniques are not able to reach low temperatures and interesting hole densities due to the "sign" problem. Nevertheless, it is possible to get useful information from exact diagonalizations on small systems using Lanczos-like techniques. These results will

be presented in detail in Sec. III. While we agree with Kane *et al.*<sup>4</sup> that there is a quasiparticle peak at the bottom of the hole spectrum, we found structure beyond it, which is well described by states of a particle in a linear confining potential like in the Ising limit. We discuss the  $J$  dependence of those levels as well as the behavior of the bandwidth and the spectral weight of the quasiparticle. Excited states are also discussed.

These numerical results can be checked by perturbation theory when  $J/t$  is large. We present this perturbation in Sec. IV. The exploration of this large  $J/t$  regime allows us to give a unified picture of the hole motion for the whole parameter space.

Finally, in Sec. V we show results for the Hubbard model on small 8 and 10 site lattices; again a quasiparticle peak is found. We analyze both the weak- and strong-coupling regions and discuss the quantum numbers of the ground state in the one-hole subspace and the quasiparticle bandwidth.

## II. ONE HOLE IN THE $t$ - $J$ MODEL; GROUND-STATE PROPERTIES

Some properties of one hole in a Heisenberg antiferromagnet are well established while others remain controversial. Using a variational method and spin-wave techniques, Siggia and Shraiman showed<sup>6</sup> that the momentum of one hole in the ground state of the  $t$ - $J$  model is  $\mathbf{k}=(\pm\pi/2, \pm\pi/2)$ , i.e., it lies on four points that belong to the Fermi surface of the Hubbard model at  $U=0$ . A similar result was obtained using different variational approaches and diagrammatic techniques.<sup>7,4,8</sup> Numerically, exact diagonalization results on 10 site lattices showed<sup>9</sup> that the momentum of the hole is  $\mathbf{k}=(3\pi/5, \pi/5)$  (plus its  $\pi/2$  rotated states) which is the closest to the noninteracting Fermi surface for that lattice. Lanczos studies on a larger lattice of 16 sites ( $4\times 4$ ) with periodic boundary conditions showed<sup>10,11</sup> that indeed the  $\mathbf{k}$  of the hole lies on that Fermi surface, but, due to a geometrical property of that lattice,  $\mathbf{k}=(\pm\pi/2, \pm\pi/2)$  and  $\mathbf{k}=(\pi, 0), (\pi, 0)$  are degenerate. The reason is well known: The  $4\times 4$  lattice is equivalent to a hypercubic  $2^4$  lattice as shown in Fig. 1. Note that while the distances between sites 1–3 and 1–6 are of 2 and  $\sqrt{2}$  lattice spacings on the  $4\times 4$  lattice, in the hypercube both are actually equivalent and that reduces the number of independent momenta by one. Then, using a  $4\times 4$  lattice and nearest-neighbor interactions, it is impossible to check which momentum corresponds to the actual minimum of the one hole band. This issue is very important in some theories of superconductivity that approach the Hubbard model from the weak coupling side.<sup>12</sup> There, depending on where on the Fermi surface “pockets” are developed (i.e., what momentum the first holes doped into the system have), the superconducting gap  $\Delta$  will have different symmetries. If the holes have  $\mathbf{k}=(\pm\pi/2, \pm\pi/2)$  then  $\Delta$  will transform like a  $p$  wave while if  $\mathbf{k}=(\pi, 0), (0, \pi)$ ,  $\Delta$  will correspond to a  $d$  wave. Only calculations on large lattices can answer that question. Lattices accessible to Lanczos studies beyond 16 sites (like 18 or 20 sites) that do not have the isomor-

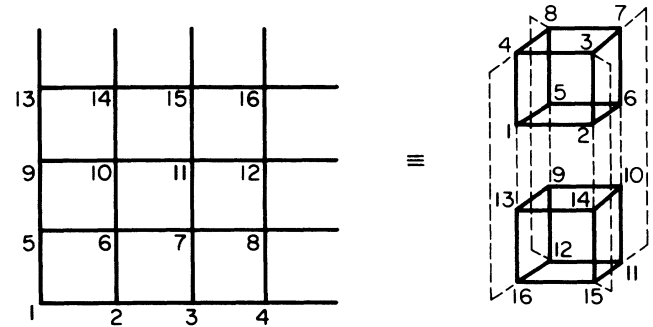


FIG. 1. Geometrical relation between the  $4\times 4$  lattice and a hypercubic  $2^4$  lattice. The dashed lines on the hypercube denote links along the 4th direction.

phism while the hypercube do not contain those interesting particular momenta. Thus one has to rely on whether the ground state has a  $\mathbf{k}$  “close” to one or the other which is a dubious procedure when such small gaps are in discussion.

Studying the Ising model with one hole ( $t$ - $J_z$  model) does not help either, in spite of the fact that for this model it is possible to do a simulation on larger lattices.<sup>13</sup> The reason is that the  $\mathbf{k}$  of the hole turns out to be  $(0,0)$  on a  $4\times 4$  lattice (as discussed in Sec. III). The results for larger lattices are very close in energy so there is no reason to suspect that a change in  $\mathbf{k}$  will result from increasing the lattice size. This shows that the quantum fluctuations are crucial to reproduce the nonzero  $\mathbf{k}$  of the hole in the  $t$ - $J$  model. A possible answer to what is the actual momentum of the hole in the bulk limit may come from the addition of small perturbations around the  $t$ - $J$  model. For example, using the extended Hubbard model it has been shown<sup>14</sup> that for a  $4\times 4$  lattice the hole has  $\mathbf{k}=(\pm\pi/2, \pm\pi/2)$ . A similar conclusion was obtained for the  $J$ - $t$ - $t'$  model.<sup>15</sup> All these results are based on strong-coupling Hamiltonians, and when the coupling  $U$  of the Hubbard model is reduced, nothing prevents a crossing of levels from  $\mathbf{k}=(\pm\pi/2, \pm\pi/2)$  to  $\mathbf{k}=(\pi, 0), (0, \pi)$ .

Another subject under current investigation in the  $t$ - $J$  and Hubbard models correspond to ferromagnetism. It was shown a long time ago by Nagaoka<sup>16</sup> that at  $J/t=0$  (or  $U/t=\infty$ ) in the Hubbard model on a square lattice, the ground state of one hole has the maximum possible spin (i.e., it is a saturated ferromagnet). The reason is that in this regime there is no cost in energy to keep the spins aligned ( $J=0$ ), while the kinetic energy of the hole is minimized by a ferromagnet [where the hole has a dispersion relation  $E(\mathbf{k})$  corresponding to that of a “free” spinless particle in a trivial tight-binding problem with  $\mathbf{k}=(0,0)$  in the ground state]. Of course, turning on  $J/t$ , the cost in potential energy grows quickly like the number of sites, while the gain in kinetic energy is only of order 1 (just one hole) and then there is a phase transition (level crossing) to the “normal” phase having the electrons coupled with minimum spin  $S=\pm\frac{1}{2}$  and, as discussed above, the momentum of the hole presumably at

$\mathbf{k}=(\pm\pi/2,\pm\pi/2)$  in strong coupling. These results have been observed very clearly in an exact diagonalization study.<sup>10</sup> Actually, the crossing from the states of maximum to minimum spins may not be abrupt but instead involves other states of intermediate spin that become the ground state in very narrow regions of parameter space.<sup>10</sup>

Does ferromagnetism survive the inclusion of more holes? This is a very controversial issue. In the ferromagnetic sector  $E(\mathbf{k})$  corresponds to that of a free spinless particle. In the two-holes subspace (and neglecting hole interactions) we can put one particle at  $\mathbf{k}=(0,0)$  while the second one necessarily needs to pay some energy due to antisymmetrization [and thus has  $\mathbf{k}=(0,2\pi/L)$ , where  $N=L^2$ ]. On the other hand, due to the degeneracy of the ground state in the  $S=\frac{1}{2}$  subspace produced by the  $\mathbf{k}\neq 0$  of the hole, in principle, one can accommodate two holes at the ground state without problems of orthogonalization. The competition between these two effects may lead to a spin of the ground state different from the maximum even at  $U=\infty$ . For two holes, this seems to be the case (as shown in Ref. 17), where two calculations were done. First, beginning with a fully saturated ferromagnet with two holes just one spin was flipped to check the stability of that state. For lattices up to  $10\times 10$  sites it was found (still at  $U=\infty$ ) that by doing so the state with spin reduced by one with respect to the saturated ferromagnet, lowered its energy while the momentum of the two-holes ground state acquired a nonzero value  $(0,\pi),(\pi,0)$ . Working with small lattices it was actually found that the ground state of the two-holes system is a singlet ( $S=0$ ).<sup>17,18</sup> What happens for a higher density of holes is not clear. Results on  $4\times 4$  lattices with many holes<sup>19</sup> suggest that for more than two holes the spin of the ground state has a nonzero value although it is not fully saturated. Thus the ferromagnetic phase may be stable after all. More work is needed to completely clarify this issue.

In the limit of large  $J/t$ , the  $t$ - $J$  model departs from the Hubbard model and it describes very heavy holes in a Heisenberg background. This special case will be discussed in detail in Sec. IV. Here we only mention that, in addition to the crossing of levels in the ground state at very small  $J/t$  due to Nagaoka's theorem, we found that the  $t$ - $J$  model on a  $4\times 4$  lattice presents additional crossings at large  $J/t$ . For example, for  $J/t > 2$  the energy is minimized by  $\mathbf{k}=(\pi/2,\pi)$  instead of  $\mathbf{k}=(\pi/2,\pi/2)$  and, for even larger values of  $J$ , there is an additional crossing of levels with the minimum now at  $\mathbf{k}=(\pi,\pi)$ . These results can be explained doing perturbation theory in  $t/J$  directly in the bulk limit.

An interesting issue that can also be discussed in the context of exact diagonalization studies is how antiferromagnetism is altered around the hole due to its presence. In the spin-bag approach<sup>12</sup> the hole reduces the staggered magnetization order parameter in its vicinity and is thus self-trapped acquiring a large effective mass. Such an effect was actually observed on a  $4\times 4$  lattice,<sup>10</sup> in the Ising model on  $8\times 8$  lattices<sup>13</sup> and in Hartree-Fock studies of the Hubbard model.<sup>20</sup> The shape of the bag around the hole was found to be cigar-like<sup>12</sup> in weak-coupling perturbation theory. That result was also

confirmed in the  $t$ - $J$  model,<sup>10</sup> where it was found that the finite  $\mathbf{k}$  of the hole is the physical origin of the shape of that distorted spin bag. In addition to the bag, recently<sup>21</sup> it has been claimed that the spins are distributed around the hole such that they present a long-range dipolar distortion which has been observed in a numerical study<sup>14</sup> of the  $t$ - $J$  model.

What do we know about binding of holes in these models? In the  $t$ - $J$  model work has been done on  $4\times 4$  lattices with many holes showing that there is actually a region where two holes prefer to be at close distance forming a bound state.<sup>9,11,18,22,23</sup> This is not surprising since at very large  $J/t$  it is clear that in order to minimize the number of broken bonds in the antiferromagnet from 8 to 7, two holes should stay at a distance of one lattice spacing. This result has been verified numerically<sup>24</sup> at  $t=0$  for large lattices up to  $8\times 8$ . Actually, for a system with many static holes the lowest energy configuration is the one where all of them form a large cluster (again to minimize the number of broken bonds) and that will certainly not correspond to a superconducting phase. Of course, the Coulombic interaction between holes has been neglected (as with electrons when they are not in the same site), but in a more realistic model it should be present since there is always a background of positive charge in any material and thus the hole effectively carries such a charge. From the competition of electric repulsion and number of broken bonds minimization, we should find the actual ground state [like in a problem of nuclear physics with electric (repulsive and long-range) and nuclear (attractive and short-range) forces].

In the one-band Hubbard model with holes there is little information for two dimensions at zero temperature. Not much numerical work has been done in this model mainly because its Hilbert space is much larger than that of the  $t$ - $J$  model. In Sec. V we will discuss for the first time the quantum numbers of one hole in the Hubbard model for small lattices as well as its dynamical properties. Only a study of the binding of holes at half-filling has been presented in the literature using a new MC method that relies on an *imaginary* chemical potential for a  $4\times 4$  lattice<sup>25</sup> (and Lanczos studies for 8 site lattices<sup>18</sup>). In Ref. 25 it was found that two holes in a half-filled system bind with a small energy of  $\Delta=-0.10t$  at  $U/t=4$ . In Fig. 2, we show that result taken from Ref. 25. Note that the minimum in  $\Delta$  is obtained in the range  $U/t\approx 4-5$ . Although there is no clear connection between the bound states of just two holes and superconductivity, Fig. 2, suggests that the interesting region of this model is the intermediate regime rather than the very-strong-coupling one ( $U/t=4$  means  $J/t=4t/U=1$  in the  $t$ - $J$  notation). In that interesting regime, the  $t$ - $J$  and Hubbard models may be very different. For example, Fig. 3 shows a comparative plot of the binding energy of two holes for both models with results taken from Refs. 25 and 18. The overlap in the negative  $\Delta$  region is small. The binding energy becomes positive (no attraction) at large  $U/t$  and that may be related with the formation of ferromagnetic polarons in that regime.

Finally, note that there is a very elegant way to study the properties of holes in the  $t$ - $J$  model which makes use

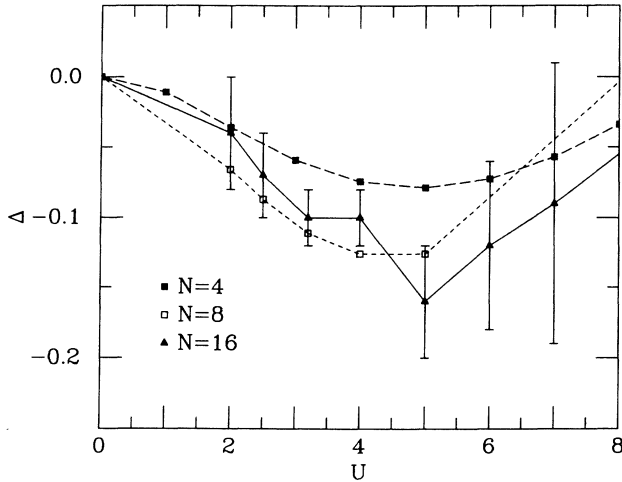


FIG. 2. Binding energy of two holes ( $\Delta$ ) as a function of  $U$  (at  $t=1$ ), for a  $4 \times 4$  one-band Hubbard model (solid line) taken from Ref. 25. The long-dashed line is the result for a  $2 \times 2$  lattice while the short-dashed line corresponds to an 8 site lattice (Ref. 18).

of gauge theories. It has been shown<sup>26</sup> that the Heisenberg model can be written as a gauge theory with local group  $SU(2)$  and massless Dirac fermions. The derivation involves the introduction of a gauge vector field to decouple the four-fermion interaction of the Heisenberg model in the path-integral formulation. The introduction of dynamical holes explicitly breaks this symmetry but the gauge formulation may still be a good starting point for this type of problems. From the numerical study described above it can be shown<sup>10,27</sup> that it is possible to derive the existence of gauge fields in a more physical

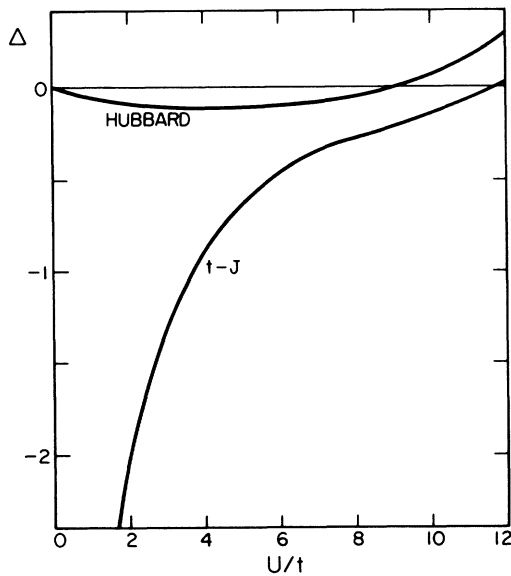


FIG. 3. Binding energy of two holes in the Hubbard and  $t$ - $J$  models as a function of  $U/t$ . The results are only approximate and taken from Refs. 25 and 18.

way as follows: Consider as an example a  $2 \times 2$  lattice and let us work at  $J/t=0$ . The one-hole sector consists of 12 states that can be decomposed into three subspaces of 4 states each corresponding to total spin  $S = \frac{3}{2}, \frac{1}{2}, \frac{1}{2}$ . The block of spin  $\frac{3}{2}$  can be immediately written as a  $4 \times 4$  matrix isomorphic to one spinless particle moving in a zero external field where  $E(\mathbf{k}) = -2t(\cos k_x + \cos k_y)$ . The other two sectors are more interesting. Let us consider a basis where the hole is fixed at some site and the remaining three spins are coupled in a doublet  $S = \frac{1}{2}$  which can be schematically represented as

$$\frac{1}{(3)^{1/2}} \left[ \begin{pmatrix} 0 & \uparrow \\ \uparrow & \downarrow \end{pmatrix} + \gamma \begin{pmatrix} 0 & \downarrow \\ \uparrow & \uparrow \end{pmatrix} + \gamma^2 \begin{pmatrix} 0 & \uparrow \\ \downarrow & \uparrow \end{pmatrix} \right], \quad (3)$$

where  $\gamma = e^{i2\pi/3}$  or  $e^{-i2\pi/3}$ . In this basis the doublet blocks can be written as

$$\begin{pmatrix} 0 & -t\gamma^* & 0 & -t\gamma \\ -t\gamma & 0 & -t\gamma^* & 0 \\ 0 & -t\gamma & 0 & -t\gamma^* \\ -t\gamma^* & 0 & -t\gamma & 0 \end{pmatrix}. \quad (4)$$

By inspection it is clear that this block corresponds to a single particle moving in a nonzero external gauge field given by  $A_{ij}$  as shown in Fig. 4. This field cannot be contracted to zero by a gauge transformation and its circulation around the plaquette gives a nonzero magnetic field. Solving the Hamiltonian Eq. (4) we find that the ground state has a finite momentum  $\mathbf{k} = (0, \pi), (\pi, 0)$ , which is the effect we wanted to investigate. This shift in  $\mathbf{k}$  is the same as the one that occurs in particles in external fields. It is also remarkable that in the doublet sectors of this tiny  $2 \times 2$  lattice we already have a drastic reduction of the bandwidth as can be seen from solving this problem exactly.

This argument may be generalizable to larger lattices. At  $J/t=0$  the block with maximum spin corresponds to that of a particle in a zero external field as we know happens in the ferromagnetic sector. Some of the blocks with minimum spin can be written in a basis which is the generalization of Eq. (3), i.e., with the hole at a given site and the spins coupled in a singlet ( $N \times N$  matrix). The coefficients of this combination of states are phases (multiplied by  $t$ ). The doublet blocks again can be mapped

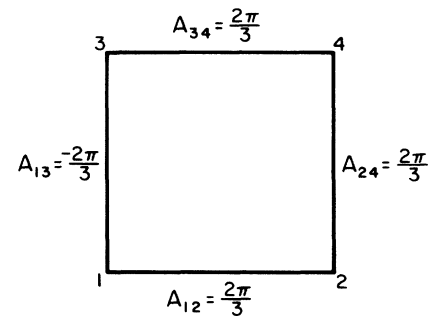


FIG. 4.  $2 \times 2$  lattice showing the fictitious gauge field introduced by the overlap of spin wave functions.

into a one-particle problem of an electron in an external field. We believe, although we do not have a proof, that in the bulk limit the external field will correspond to a uniform magnetic field of flux  $\pi$  per plaquette which gives a minimum energy at  $\mathbf{k}=(\pm\pi/2, \pm\pi/2)$ . Such a result would introduce a nice connection with the flux phase<sup>28</sup> which is known to have that momentum in the one-hole sector.

### III. ONE HOLE IN THE $t$ - $J$ MODEL: DYNAMICAL PROPERTIES

#### A. Numerical method

In this section we present results for the spectral function  $S(\mathbf{k}, \omega)$  of one hole with momentum  $\mathbf{k}$  and energy  $\omega$  (with respect to the ground state of zero holes) in the  $t$ - $J$  model. Results for the Hubbard model will be presented in Sec. V.  $S(\mathbf{k}, \omega)$  is important for the analysis of dynamical properties of these systems. The first numerical study of  $S(\mathbf{k}, \omega)$  for the  $t$ - $J$  model was presented by Dagotto *et al.*<sup>29</sup> and later independently by Stephan *et al.*<sup>30</sup> An analysis of  $S(\mathbf{k}, \omega)$  was recently reported by Trugman<sup>31</sup> using a new variational technique with results very close to those of Ref. 29. Recently, an analysis of  $S(\mathbf{k}, \omega)$  for the two-band Hubbard model (in strong coupling) has also been presented.<sup>32</sup>

To study  $S(\mathbf{k}, \omega)$  numerically we used the identity

$$S(\mathbf{k}, \omega) = -\text{Im}[G(\mathbf{k}, \omega + E_0 + i\epsilon)], \quad (5)$$

where  $G(\mathbf{k}, x) = \langle \psi_0 | \bar{c}_{\mathbf{k}, \sigma}(x - H)^{-1} \bar{c}_{\mathbf{k}, \sigma}^\dagger | \psi_0 \rangle$  and  $\bar{c}_{\mathbf{k}, \sigma}^\dagger = \sum_i e^{i\mathbf{k} \cdot \mathbf{r}_i} \bar{c}_{i, \sigma}^\dagger$ , i.e., the spectral function can be related to the imaginary part of the retarded Green's function of a hole. For simplicity we only consider hole operators with spin up and thus the spin index is dropped from now on.  $|\psi_0\rangle$  is the ground state of the Heisenberg model for zero hole (having energy  $E_0$ ) which we obtained using the modified Lanczos method and has been described in detail in previous papers.<sup>33</sup> Note that this state is  $J$  independent in the Heisenberg model. Our results below crucially depend on the properties of  $|\psi_0\rangle$ .  $\epsilon$  is a small parameter that gives a finite width to the  $\delta$  functions appearing at each pole of  $G$  (it shifts the poles from the real axis). Any state of the one-hole subspace which has a nonzero projection over the state  $|1\rangle = \bar{c}_{\mathbf{k}}^\dagger |\psi_0\rangle$  will contribute to the spectral function. Note that using Eq. (5) we only need to evaluate matrix elements of appropriately chosen operators in the state  $|1\rangle$ . Then, we actually never explicitly obtain all the excited states of the one-hole sector as naively required to calculate a spectral function.

In the calculation of  $S(\mathbf{k}, \omega)$  it is important to note that  $G$  admits a continued fraction expansion<sup>34,35</sup> as

$$G(\mathbf{k}, x) = \frac{1}{x - a_0 - \frac{b_1^2}{x - a_1 - \frac{b_2^2}{x - a_2 - \dots}}} \quad (6)$$

We know that  $G$  has poles only on the real axis and Eq. (6) has this property.<sup>36</sup> The coefficient  $a_m, b_m$  appearing

in Eq. (6) are functions of the matrix elements  $\langle 1 | H^n | 1 \rangle$  ( $n = 1, \dots, m$ ), where  $|1\rangle$  is the state of one hole. These matrix elements can be evaluated numerically for increasing  $m$  by using the modified Lanczos program. The coefficients  $a_m, b_m$  can be obtained recursively using the formulas,

$$\begin{aligned} a_n &= \langle f_n | H | f_n \rangle / \langle f_n | f_n \rangle, \\ |f_{n+1}\rangle &= H |f_n\rangle - a_n |f_n\rangle - b_n^2 |f_{n-1}\rangle, \\ b_{n+1}^2 &= \langle f_{n+1} | f_{n+1} \rangle / \langle f_n | f_n \rangle, \end{aligned} \quad (7)$$

where  $b_0^2 = 0$ ,  $n = 0, 1, 2, \dots$ ,  $|f_{-1}\rangle = 0$  and as initial state we take  $|f_0\rangle = |1\rangle$ . This procedure has been applied to the one-dimensional Heisenberg model with excellent results.<sup>37</sup> In this paper and in Ref. 29 we have shown that the method can be extended to fermionic systems without any additional problems. To stop the iterations we have not used a special method but we simply constructed  $S(\mathbf{k}, \omega)$  explicitly for different values of  $m$  until convergence was observed. In general, the dominant peaks are the first to appear and their positions and weights are accurately obtained after a few iterations, while for the peaks with lower intensity more iterations are needed. A typical number of iterations used in our results below ranges between 80 and 300 iterations (since the one-hole Hilbert space of the  $4 \times 4$  lattice contains 6435 states, then there are no additional problems by performing this large number of iterations).

To check our program we reproduced the ground-state hole energies previously obtained by the Lanczos method,<sup>10</sup> and we also verified that the standard sum rule coming from the integration over  $\omega$  of the spectral function,

$$\int d\omega S(\mathbf{k}, \omega) = \frac{\pi N}{2}, \quad (8)$$

is satisfied. For large  $J/t$  the ground-state energy is accurately obtained after very few iterations showing that the state  $|1\rangle$  (basically a hole in an undisturbed spin background) is a good approximation to the ground state. Actually, if  $|1\rangle$  is used as the starting configuration of the modified Lanczos method, the rate of convergence is also greatly improved. For small  $J/t$  the convergence rate decreases since the hole appreciably perturbs the surrounding spins.

We end this subsection with a comment about fermions in the  $t$ - $J$  model. In the one-hole sector it is possible to work ignoring the fact that the spins are actually fermionic particles (this cannot be done for more than one hole). To show this, consider a  $4 \times 4$  lattice with periodic boundary conditions with the sites of the lattice ordered in a "one-dimensional" pattern as shown in the  $4 \times 4$  lattice of Fig. 1. This means that a state corresponding to a hole in site 5, for example, and the spins in some arbitrary state is described by the ket

$$c_{16}^\dagger \cdots c_6^\dagger c_4^\dagger \cdots c_1^\dagger |0\rangle, \quad (9)$$

where the spin index is not explicitly shown since it is not important for the argument below. In general, the order of the fermions matter due to the appearance of minus

signs when the particles anticommute. This is not a problem for the Heisenberg term that always involves two fermionic operators at the same site, but it is important for the hopping term. When the hopping term acts in the  $y$  direction, due to the one-dimensional arrangement of spins we used, there is always a minus sign since an electron needs to “jump” over three other electrons in the state, Eq. (9), to move one unit in the  $y$  direction (for more than one hole this number changes from configuration to configuration); then the  $y$  hopping effectively changes sign. In the  $x$  direction there is no sign problem except at the boundary: When the fermions or hole at sites 4, 8, 12, and 16 move to the first row another minus sign appears in the problem. Actually, it can be shown that changing from a bosonic to a fermionic representation corresponds to a global change of sign of  $t$  and thus to a shift in  $(\pi, \pi)$  of the momenta of the eigenstates as the only consequence of using one convention or the other. Other effects of this change of representation have been discussed in the Hubbard model.<sup>38</sup>

### B. Results and interpretation

In Fig. 5 we show the spectral function of one hole with  $\mathbf{k}=(\pi/2, \pi/2)$  for values of  $J/t=2.0, 1.0, 0.7, 0.4, 0.2, 0.1,$  and  $0.0$ . This value of  $\mathbf{k}$  was selected because the ground state of one hole has that momentum on a  $4 \times 4$  lattice [degenerate with  $\mathbf{k}=(\pi, 0), (0, \pi)$ ] at least in the physically interesting range of  $J/t$  [for very small  $J/t$  the ferromagnetic state with zero momentum is the ground state, while for very large  $J/t$  the ground state has  $\mathbf{k}=(\pi, \pi)$ ]. The energy of a hole with respect to the zero-hole ground state (i.e., the position of the first peak in Fig. 5) is presented in Table I, while the  $\mathbf{k}$  dependence of that peak is shown in Table II.

In Fig. 6 and Tables III and IV we show similar information, but for the special case of the Ising model with one hole (that we call the  $t$ - $J_z$  model) we compare with the  $t$ - $J$  model [the one-hole ground state now has  $\mathbf{k}=(0, 0)$ ]. In this case the Hamiltonian is

$$H = J_z \sum_{i, \hat{\delta}} S_i^z S_{i+\hat{\delta}}^z - t \sum_{i, \hat{\delta}, \sigma} (\bar{c}_{i, \sigma}^\dagger \bar{c}_{i+\hat{\delta}, \sigma} + \text{H.c.}), \quad (10)$$

i.e., it differs from the  $t$ - $J$  model in the spin-spin interac-

TABLE I. Energy of one hole in the  $t$ - $J$  model (at  $t=1$ ) on a  $4 \times 4$  lattice as a function of  $J$ . The hole state has  $\mathbf{k}=(\pi/2, \pi/2)$ .

$J$	$E_h$
0.20	-2.298
0.30	-1.997
0.40	-1.722
0.55	-1.344
0.70	-0.993
1.00	-0.345
1.50	0.632
2.00	1.527
5.00	6.24
20.00	26.88

TABLE II. Energy of one hole in the  $t$ - $J$  model (at  $t=1$ ) on a  $4 \times 4$  lattice for different momenta ( $\mathbf{k}$ ).

$\mathbf{k}$	$J=0.2$	0.4	0.7	1.0
(0,0)	-2.028	-1.055	0.045	0.849
$(\pi/2, 0)$	-2.135	-1.461	-0.648	0.043
$(\pi/2, \pi/2)$	-2.298	-1.722	-0.993	-0.345
$(\pi/2, \pi)$	-2.197	-1.582	-0.856	-0.236
$(\pi, \pi)$	-2.052	-1.134	-0.110	0.509

tion which now involves only the  $z$  component. The rest of the notation is as in Eq. (1). As state  $|\psi_0\rangle$  in Eq. (5), we take the Néel state which is the exact ground state at  $t=0$ .

Some features of the result shown in Fig. 5 are evident. (i) For a wide range of values of  $J/t$  there is a large peak at the bottom of the spectrum. We identify this peak with the quasiparticle predicted in Ref. 4. Later we will find that indeed this quasiparticle has a finite bandwidth and it thus seems to move coherently like a particle with a renormalized mass (we do not have information yet about the renormalized spin and charge which may involve large distance effects). The reason for the existence of a stable quasiparticle is related to the density of states of low-energy spin-waves which is linear in the energy.<sup>4</sup> (ii) At large  $J/t$  ( $\geq 2$ ), there is a very clear dominant peak corresponding to the ground state of the system where the hole is almost static (we will denote this limit as the “static” limit). Only a couple of additional peaks can be observed in addition to the first one with the resolution used in Fig. 5 ( $\varepsilon=0.1$  and  $\Delta\omega=0.02$ ). Increasing that resolution many more peaks were found at much higher energies but with negligible spectral weight. The total width of the spectrum grows like  $J$  in this limit. (iii) Reducing  $J/t$ , the main peak reduces its height (losing spectral weight) while the other two peaks are broader and closer in energy. At  $J/t=0.2$  the dominant peak can still be clearly seen but now additional structure appears in the problem. After that peak there is a small gap separating it from a broadband containing many states

TABLE III. Energy of one hole in the  $t$ - $J_z$  model (at  $t=1$ ) on a  $4 \times 4$  lattice as a function of  $J_z$ . The hole state has  $\mathbf{k}=(0, 0)$ .

$J_z$	$E_h$
0.00	-4.000
0.20	-2.754
0.40	-2.072
0.50	-1.805
0.60	-1.561
0.70	-1.333
0.75	-1.225
1.00	-0.723
1.50	0.137
2.00	0.882
5.00	4.486
20.00	19.867

TABLE IV. Energy of one hole in the  $t$ - $J_z$  model (at  $t=1$ ) on a  $4\times 4$  lattice for different momenta ( $\mathbf{k}$ ).

$\mathbf{k}$	$J_z=0.2$	0.4	0.7	1.0	2.0
(0,0)	-2.754	-2.072	-1.333	-0.723	0.882
$(\pi/2,0)$	-2.601	-1.993	-1.293	-0.702	0.886
$(\pi/2,\pi/2)$	-2.544	-1.959	-1.278	-0.695	0.887
$(\pi/2,\pi)$	-2.613	-1.994	-1.293	-0.702	0.886
$(\pi,\pi)$	-2.698	-2.069	-1.333	-0.723	0.882

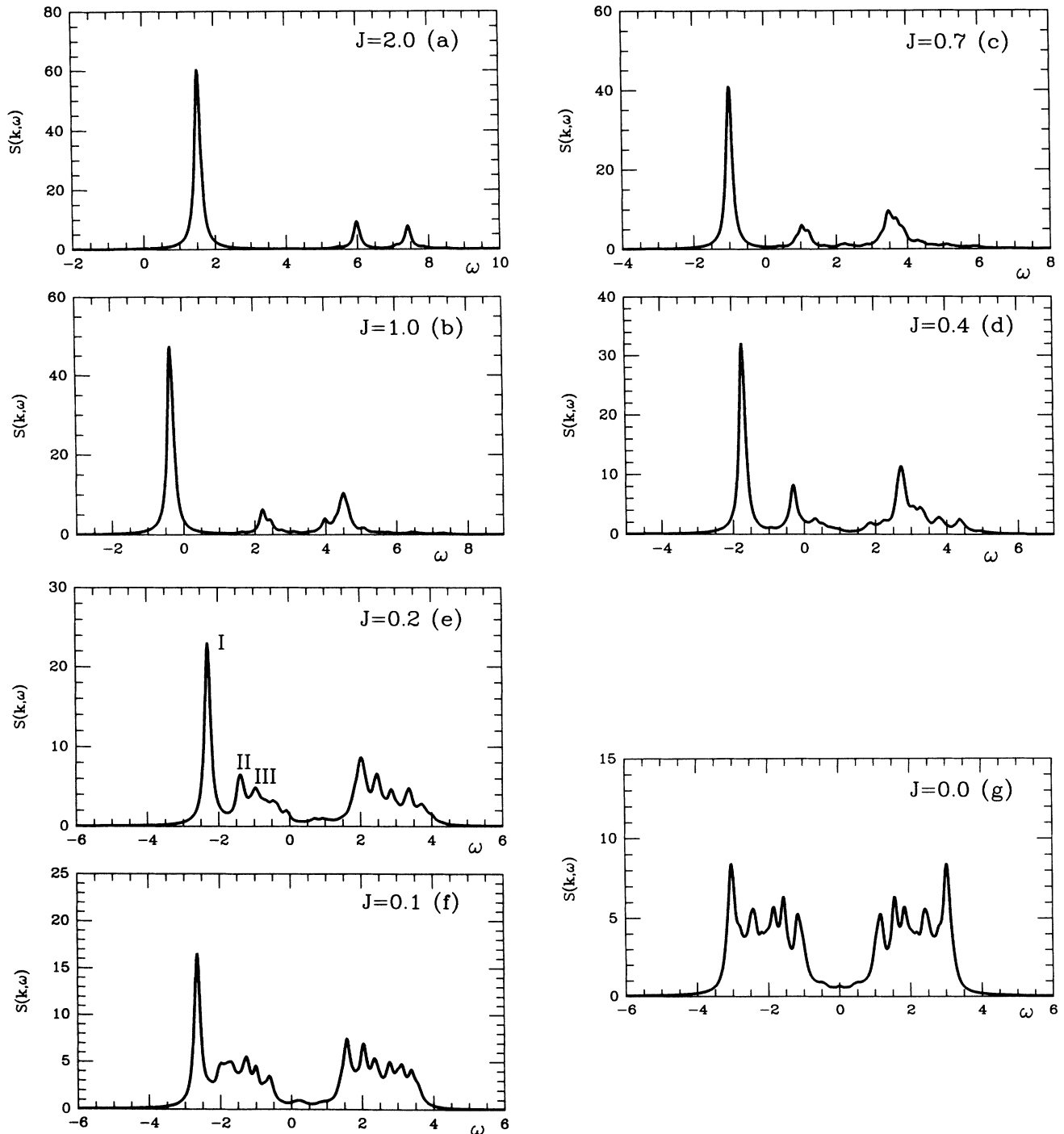


FIG. 5. Spectral function of one hole in the  $t$ - $J$  model at  $\mathbf{k}=(\pi/2,\pi/2)$  for different values of  $J$ : (a)  $J=2.0$ ; (b)  $J=1.0$ ; (c)  $J=0.7$ ; (d)  $J=0.4$ ; (e)  $J=0.2$ ; (f)  $J=0.1$ ; (g)  $J=0.0$  ( $\varepsilon=0.1$ ).

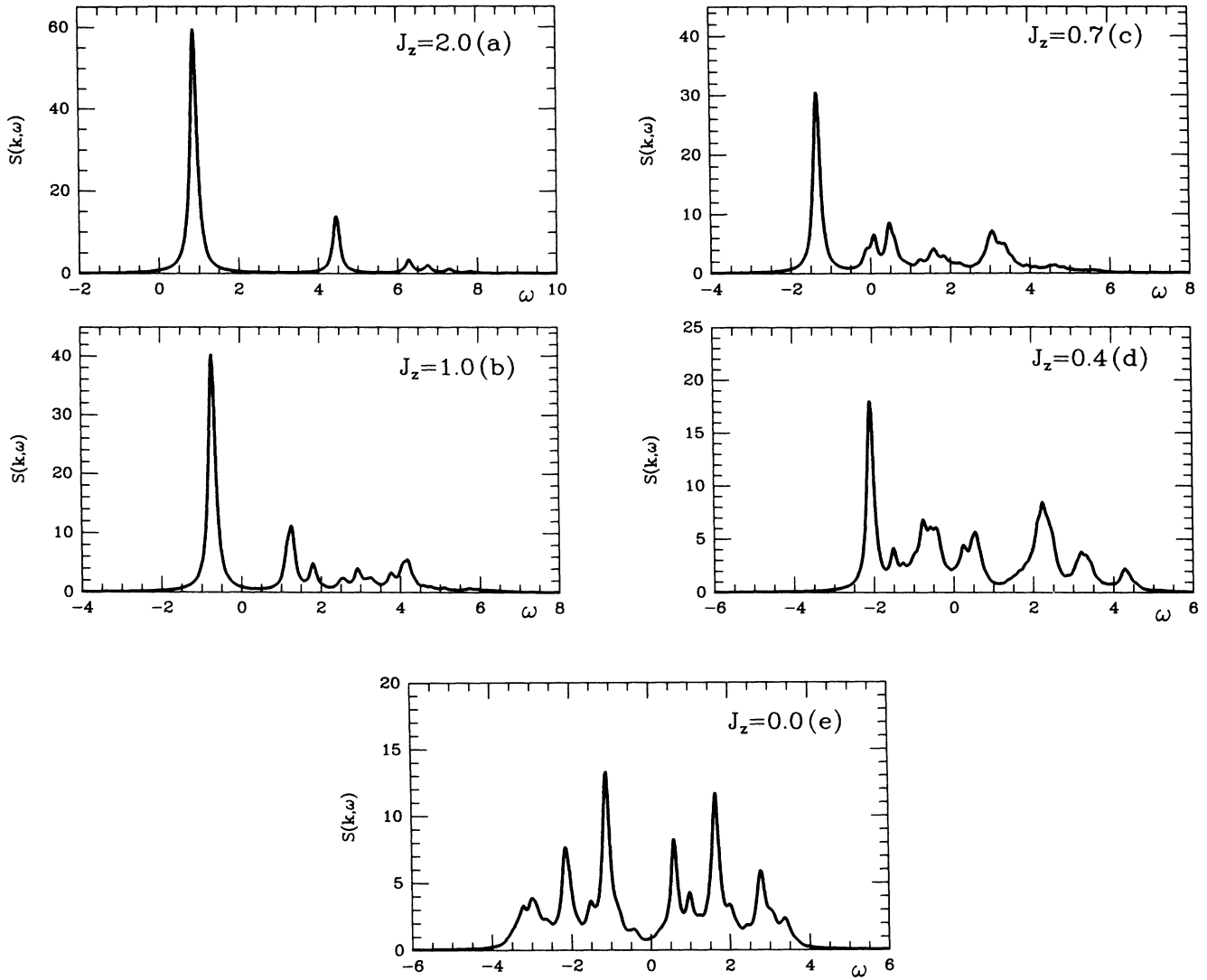


FIG. 6. Spectral function of one hole in the  $t - J_z$  model at  $\mathbf{k} = (0,0)$  for different values of  $J_z$ : (a)  $J_z = 2.0$ ; (b)  $J_z = 1.0$ ; (c)  $J_z = 0.7$ ; (d)  $J_z = 0.4$ ; (e)  $J_z = 0.0$  ( $\epsilon = 0.1$ ).

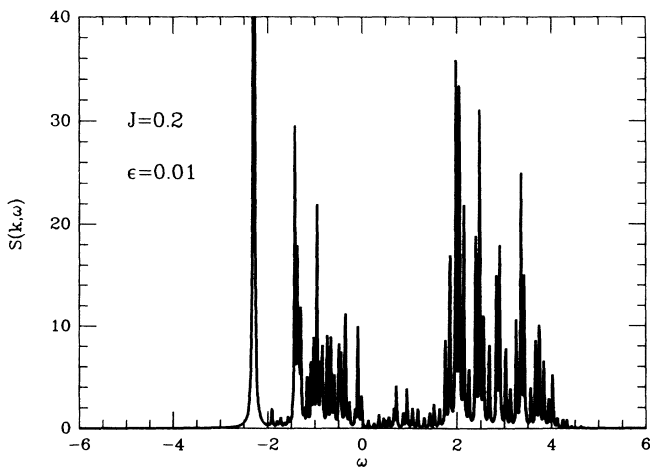


FIG. 7. Same as Fig. 5(e) but with  $\epsilon = 0.01$ .

and presenting modulated structure (note that this small gap is not present in the results of Kane *et al.*, where their incoherent band begins immediately after the quasiparticle peak). For even larger  $\omega$  another broader gap separates this band from a second one having similar characteristics. In Fig. 7 we reduced  $\epsilon$  of Fig. 5(e) from 0.1 to 0.01 in order to observe more clearly the number of peaks and gaps. Many interesting details can be observed in Fig. 7: The gaps are actually pseudogaps having states in between but with very small spectral weight. In the two broadbands all the states are not equivalent but there is a hierarchy where a few peaks are dominant, while many others appear between them with very small spectral weight. (iv) At  $J/t = 0$  the quasiparticle peak is no longer dominant (actually at very small  $J/t$  we have observed states of very low intensity crossing with the quasiparticle state and becoming the actual ground state). We found that the first pole in Fig. 5(g) is located at

around  $\approx -3.40$  which is in good agreement with the result  $-3.34$  of Joynt<sup>39</sup> and also with the result of Brinkman and Rice<sup>5</sup>  $-2\sqrt{3} \approx -3.46$  in the self-retracing approximation. The fact that this lowest energy pole is not at  $\omega = -4$  is because we are working in the subspace with  $S = \frac{1}{2}$  as is explained later. It is an interesting feature of this  $S = \frac{1}{2}$  sector that there is a reduction of the total width of the hole spectrum as was predicted in Ref. 5 and confirmed in this numerical calculation. This reduction comes from the overlap of spin-wave functions when a

hole moves.

It is important to remark that for very small  $J/t$  the actual ground state is ferromagnetic, i.e., there are a sequence of level crossings around  $J/t \approx 0.075$  on a  $4 \times 4$  lattice where the ground state of one hole changes from a doublet  $S = \frac{1}{2}$  to a higher spin state. However, our state  $|1\rangle$  used for the spectral function has spin  $\frac{1}{2}$  since the ground state of zero hole is a singlet and  $c$  is a spin  $\frac{1}{2}$  operator and, thus, states with higher spin do not appear in this spectral function [they can be easily obtained,

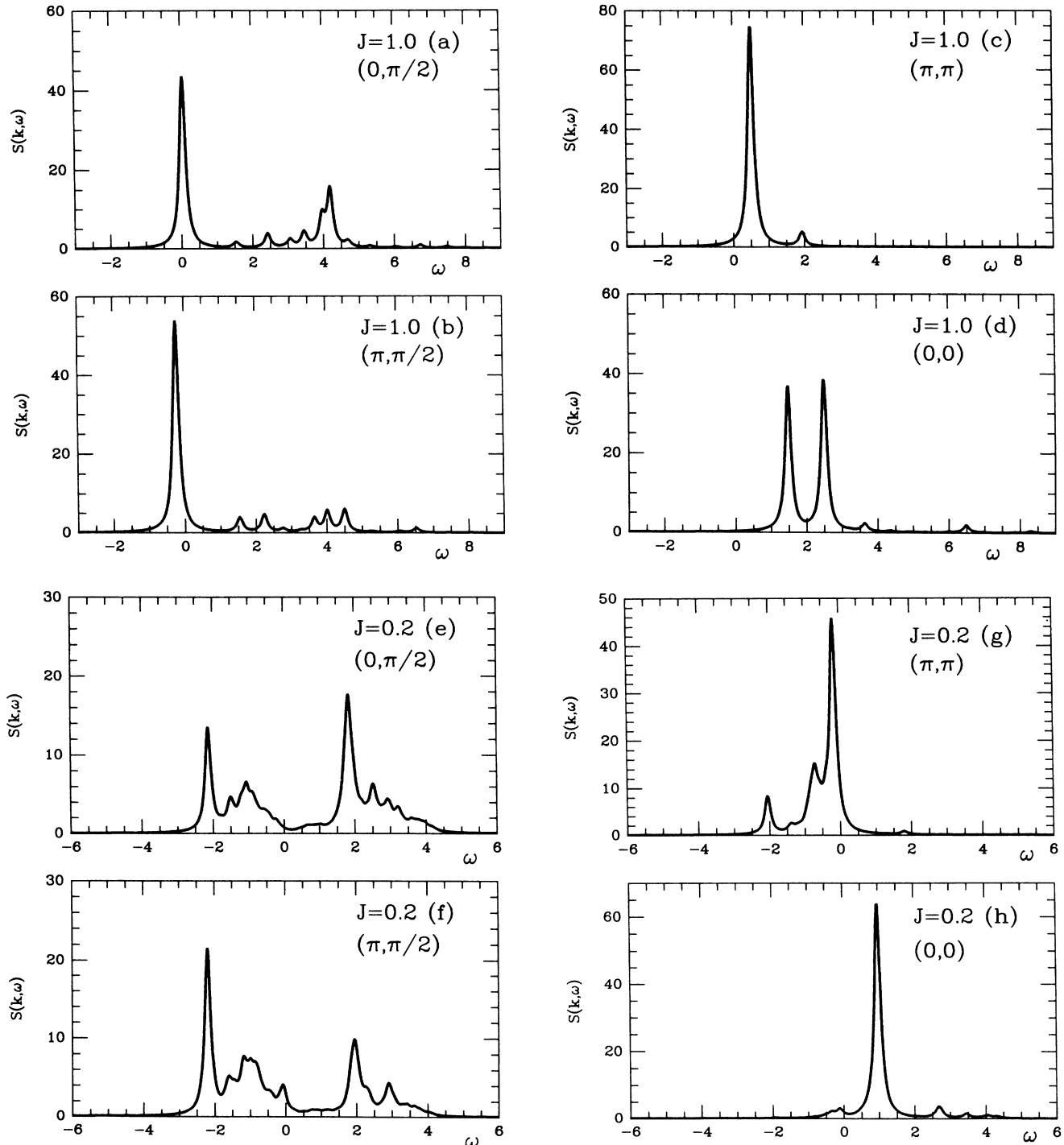


FIG. 8. Spectral function of one hole in the  $t$ - $J$  model at  $J=0.2$  and  $1.0$  for different values of  $\mathbf{k}$ .

if necessary, just changing  $|\psi_0\rangle$  in Eq. (5) to a state with higher spin]. Our results then always correspond to the doublet subspace which is the physically interesting one.

Now we analyze the momentum dependence of our results. In Fig. 8 we show  $S(\mathbf{k}, \omega)$  at  $J/t=1.0$  and  $0.2$  for the other four independent momenta  $\mathbf{k}$  of the  $4\times 4$  lattice not shown in Fig. 5. One detail is immediately obvious: The states with  $\mathbf{k}=(\pi/2, \pi/2)$ ,  $\mathbf{k}=(\pi/2, 0)$ ,  $\mathbf{k}=(\pi, \pi/2)$ , and their  $\pi/2$  rotated states (14 in total) have a very similar structure specially at small  $J/t$ , i.e., there is a clear dominant peak at the ground state followed by a tiny gap, a broadband with structure, a large gap, and finally another broadband. However, for  $\mathbf{k}=(\pi, \pi)$  and  $\mathbf{k}=(0, 0)$  the situation is very different (specially at  $J=0.2$ ): The states with lowest energies have small spectral weight while in both cases there seems to exist a dominant state at intermediate energy. This situation holds for a wide range of values of  $J/t$ . We do not have a complete explanation for the disappearance of the large quasiparticle peak at the bottom of the spectrum, but we think it is related with the quantum numbers under rotation of the state  $|1\rangle$ . For example, using a Lanczos technique we found that the ground state of the  $S=\frac{1}{2}$  sector with  $\mathbf{k}=(0, 0)$  is *odd* under a  $\pi/2$  rotation while  $|1\rangle$  is *even*. That state does not appear in the spectral function defined as in Eq. (5). This problem already appears on a  $2\times 2$  lattice which can be solved analytically. A more general definition with a hole operator spread over a few lattice sites, rather than concentrated at one site, would make that state appear in the spectral function.

In Fig. 6 we observe that the Ising model at  $\mathbf{k}=(0, 0)$  does not have the same problem as the Heisenberg model for the same momentum. There must have been a level

crossing in this subspace as a function of the perpendicular coupling (that interpolates between Ising and Heisenberg limits) from an *s*-wave (Ising) to *d*-wave (Heisenberg) state. This result, plus the change in momentum of the ground state, show that the interpolation between the two models is not smooth. For the momentum dependence of the results for the Ising model we only show a few examples in Fig. 9. Actually,  $\mathbf{k}=(0, 0)$  and  $(\pi, \pi)$  are very similar and they are now the two lowest states in the one-hole band. The rest of the band states also have very similar spectral functions, thus we show only one as a representative.

Is it possible to understand at least part of the complicated spectrum found in Fig. 5 (Fig. 6)? For that purpose it is convenient to find the dependence of the hole energy using Table I (III) with  $J$  ( $J_z$ ). We will discuss three cases separately.

(i) For  $J/t$  large (say,  $J/t > 2$ ), the quasiparticle peak corresponds to an almost static hole (actually for the Heisenberg model the bandwidth does not reduce to zero; that effect is discussed in Sec. IV) and all the energies grow like  $J$ . The excitations at high energy can be understood from the Ising limit. In this case the first excitation above the Néel state with one hole corresponds to the flip of a spin at one of the four sites surrounding the hole. Such a change in  $S^z$  is not allowed by our Hamiltonian but the excitation can be thought of differently as a distortion of the Néel state created by a hole when it moves one lattice spacing from its original position (Fig. 10). This first excitation is like a “string” of unit 1 in the language of Ref. 40. The next excitation will correspond to a string of length two, and so on. Working at  $J_z/t$  very large in the  $t$ - $J_z$  model we clearly identified these excitations numerically. Following these states to  $J_z=2$  we found that the second (third) important peak of Fig. 6(a) actually corresponds to the string of length one (two). Since the results for the Heisenberg model are qualitatively similar to the Ising model, we think that the two peaks observed in Fig. 5(a), beyond the quasiparticle, should be identified with those excitations.

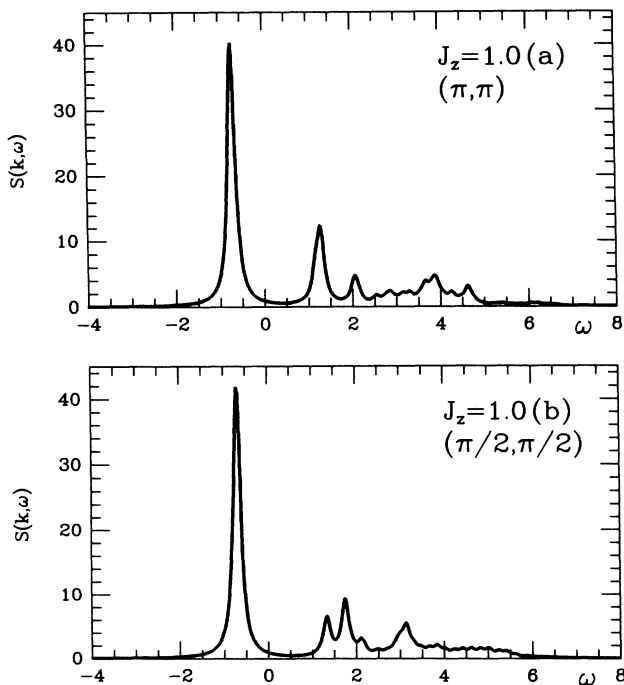


FIG. 9. Spectral function of one hole in the  $t$ - $J_z$  model at  $J_z=0.4$  and  $1.0$  at different values of  $\mathbf{k}$ .

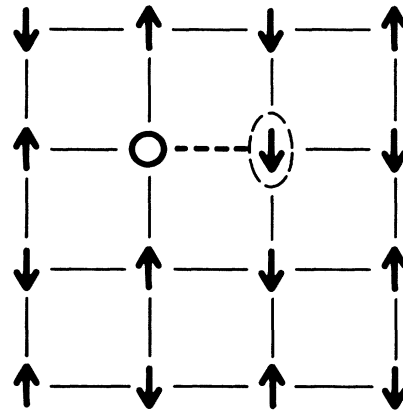


FIG. 10. Schematic representation of an excitation of one hole in the  $t$ - $J$  model at large  $J/t$ . The open circle denotes the hole and the dashed line the string of unit one. The circled spin down is overturned with respect to the Néel background.

We remark again that in this limit there is a ‘‘duality’’ of language in describing the excitations: They can be thought of as a spin flip near the almost static hole (or a spinwave trapped near the hole in the Heisenberg model) or as a string created by the hole movement distorting the N el background.

(ii) In the intermediate region  $0.2 \leq J \leq 1.0$  the energy of the quasiparticle [peak I in Fig. 5(e)] can be fit with high accuracy by a power law as  $E_h = -3.17 + 2.83J^\alpha$ , where  $\alpha \approx 0.73$ . The second peak [labeled II in Fig. 5(e)] follows a similar behavior with an energy well approximated by  $E_h = -3.13 + 5.36J^\alpha$  with  $\alpha \approx 0.70$ . Actually, a third peak [III in Fig. 5(e)] can be distinguished from the background in a narrow interval of  $J$  ( $0.2 \leq J \leq 0.4$ ) and its energy behaves as  $E_h = -3.23 + 6.26J^{0.63}$ , although this fit is less accurate than the two previous ones. The behavior of these energies is shown in Fig. 11.

We have also obtained the  $J$  dependence of the quasiparticle peaks at different  $\mathbf{k}$  values. The results are as follows. For  $\mathbf{k} = (\pi, \pi/2)$ ,  $E_h = -3.34 + 3.10J^{0.62}$ , while for  $\mathbf{k} = (\pi/2, 0)$  the energy is  $E_h = -3.346 + 3.390J^{0.64}$ . These fits work very well in the region  $0.2 \leq J \leq 1.0$ . On the other hand, it was more difficult to fit the remaining two momenta. Only for  $0.1 \leq J \leq 0.4$  we found a good power-law behavior. For  $\mathbf{k} = (\pi, \pi)$ ,  $E_h = -3.35 + 4.50J^{0.77}$ , while for  $\mathbf{k} = (0, 0)$  the result was  $E_h = -3.38 + 4.76J^{0.78}$ . Note that all of them present a power-law behavior with an exponent systematically smaller than 1 and close to each other.<sup>41</sup>

We think that the power-law behavior found for these peaks can be understood in the context of the string picture developed by Siggia and Shraiman<sup>40</sup> for the Ising model. In that case the hole distorts the spin background when it moves creating a ‘‘string’’ of overturned spins. At least for small  $J_z$ , it is possible to write an effective Hamiltonian for the hole that corresponds to a nonrelativistic particle in a linear potential having Airy functions

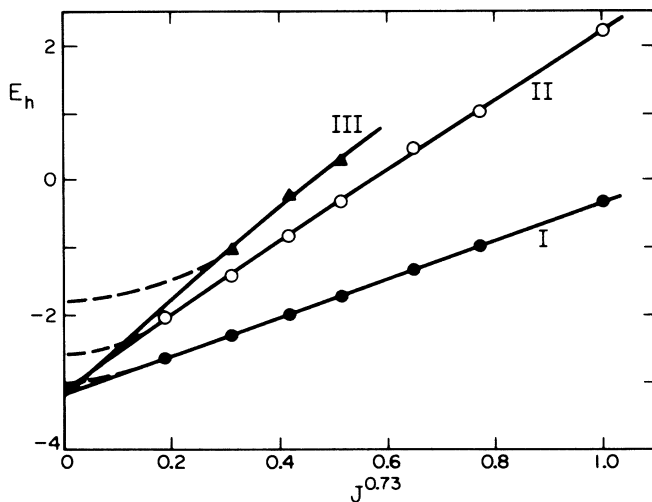


FIG. 11. Energy of the first three levels (I, II, and III) of Fig. 5(e) [ $t$ - $J$  model with  $J/t = 0.2$ , and  $\mathbf{k} = (\pi/2, \pi/2)$ ] as a function of  $J^{0.73}$ . The continuous line is the fit of the data described in the text while the dashed line is the actual behavior of the peaks due to the finite size of the system.

as eigenfunctions. The  $J_z$  dependence of the eigenvalues of this problem can be obtained exactly by a change of variables and it corresponds to  $J^{2/3}$ , which is very close to the power laws we found numerically. One may think that the spin fluctuations of the Heisenberg model would ‘erase’ this string, but our results show that at least for the first levels this is not true. Note also that at large  $J/t$  we manage to identify the first peak beyond the quasiparticle precisely as a string of length one. By continuity it is not surprising that a similar explanation may survive the reduction of  $J/t$ .

However, note that from calculations such as those presented by Siggia and Shraiman<sup>40</sup> in the Ising limit we cannot directly show the  $k$  dependence of the results found above. We believe that this dependence may be understood as follows. The hole should be thought of as a spin bag having a fermion (hole) trapped inside a confining potential. The whole configuration moves with a large mass as discussed below which contributes with a  $k^2/2m_{\text{eff}}$  term to the total energy, while the energy of the hole inside the bag is given by the levels of a particle in an external linear potential (only quantized energy levels). Then as long as the center of mass energy is small (large effective mass  $m_{\text{eff}}$ ) then the  $J$  dependence of the results is given by  $J^\alpha$  with  $\alpha \approx 0.66$  for all values of  $\mathbf{k}$ .

As a further test of the string picture note that the slopes we found in the fit  $E_h$  versus  $J^\alpha$  (i.e., 2.83, 5.36, and 6.26) are in good correspondence with the first eigenvalues of the Airy equation (i.e., 2.33, 4.08, and 5.52) specially if ratios are taken. Note also that if these levels correspond to those of a particle in a linear potential it is clear that they should converge to the same value at  $J=0$ . This coincidence should be searched for using the fits in the intermediate region and not the actual numerical results at  $J=0$  which are contaminated by finite-size effects as shown below. The numbers at  $J=0$  coming from the fits are  $-3.17$ ,  $-3.13$ , and  $-3.23$ , all of them in excellent agreement.

We found that even the first peak located after the broad pseudogap seems to follow a power-law behavior with  $\alpha$  close to 0.7 (although with bigger error bars). This peak is particularly interesting since its intensity is high compared to the rest and it behaves like a quasiparticle itself for small  $J$  (although with a finite lifetime). Possible experimental signatures of such a peak are under consideration but, of course, since it lies at high energies it may be a spurious finite-size effect. Note that the existence of this peak and corresponding band is not predicted by the string picture. It would be important to find whether it corresponds to a spurious result or not.

(iii) The results for  $J/t = 0$  require a special discussion [Fig. 5(g)]. The reflection symmetry  $\omega \rightarrow -\omega$  can be easily understood as follows. At even sites of the lattice one can make the transformation  $c_{i,\sigma} \rightarrow -c_{i,\sigma}$ . This corresponds to an effective change of sign of the hopping parameter  $t$  and thus it is equivalent to a shift in  $(\pi, \pi)$  of the momentum of the hole. For  $\mathbf{k} = (\pi/2, \pi/2)$  that shift implies just a rotation of  $\mathbf{k}$  and thus the spectral function is unchanged. In general, the relation is  $S(\mathbf{k}, \omega) = S[\mathbf{k} + (\pi, \pi), -\omega]$ . Another interesting feature of Fig. 5(g) is the appearance of a clear pseudogap around  $\omega = 0$ .

Note that in the Ising limit this pseudogap is replaced by a large peak as shown in Fig. 12. The  $t$ - $J$  and  $t$ - $J_z$  models have the same Hamiltonian in this limit but their spectral functions are not equal since  $|\psi_0\rangle$  for both cases is not the same. The origin of the new large peak of Fig. 12 are the states not present in the  $S=\frac{1}{2}$  subspace of the Heisenberg model (for example, on a  $2\times 2$  lattice the same effect clearly appears and there the peak is due to the state of maximum  $S^z$ ). Ferromagnetic states may now fill the pseudogap in Fig. 5(g). Note that this pseudogap at small  $|\omega|$  in the Heisenberg model at  $J/t=0$  is the origin of the large pseudogap observed in Fig. 5(e) ( $J/t=0.2$ ). Note also that both Figs. 5(g) and 12 show structure (peaks) on top of a mostly incoherent spectrum. For reasons discussed below, we think that this is a finite-size effect and that in the bulk limit at  $J/t=0$ , the spectral function of the Heisenberg model in the  $S=\frac{1}{2}$  sector will present just two broad incoherent bands with a strong depletion in the middle.

It is very important to discuss the influence of the finite size of our lattice in our conclusions about the string picture. For example, we know that at  $J/t\approx 0.075$  there is a crossing of levels towards the ferromagnetic phase. This is clearly a finite-size effect, therefore results for smaller  $J/t$  are not reliable. It is also important to know when the size of the “renormalized” hole (or spin bag) is comparable to the size of the lattice. From the Ising limit<sup>40</sup> we know that the size of the lowest state scales as  $1.43/J^{0.33}$  which is equal to 4 (size of our lattice) for  $J/t\approx 0.05$ . Of course the formula obtained in the Ising limit is actually asymptotic and is valid for small  $J$  and a long string so it is not clear that it is applicable to our case but at least it suggests that only for very small  $J$  we have strong finite-size effects (in agreement with the “ferromagnetic” criterion described above). Other arguments also in agreement with these results are the following. In Fig. 11 we observe that the first three dominant peaks of the problem follow very similar power-law behaviors compatible with the string picture in a broad range of parameter space, but at small  $J/t$  they deviate

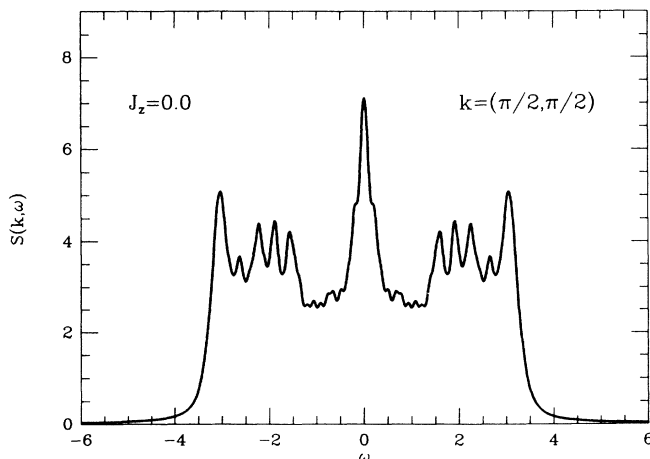


FIG. 12. Spectral function of the  $t$ - $J_z$  model at  $J_z/t=0$  and  $\mathbf{k}=(\pi/2, \pi/2)$ .

from it and each one converges to a different constant. This is the reason why at  $J/t=0$  we still find structure on top of the incoherent band. We think that the point where deviations from the asymptotic formula occurs signal the presence of finite-size effects. Note in Fig. 11 that the peaks III and II are more affected by this effect than the first one. This is reasonable because the ground state has the smallest size. Then, again we see that only for very small  $J/t$  the size of the lattice matters.

Some of us have studied the Ising model<sup>13</sup> on a  $4\times 4$  lattice and also in larger lattices of  $8\times 8$  sites. We found there that for  $0.4\leq J\leq 1.0$  the energies of both lattices are very close to each other. Actually, the asymptotic behavior that we would have deduced from the  $4\times 4$  lattice in that region would have been an excellent approximation to the results for the  $8\times 8$  lattice. In Fig. 13 we plot the energy of one hole ( $E_h$ ) for the Heisenberg model on a  $4\times 4$  lattice and the Ising model on an  $8\times 8$  lattice; the similarity is obvious. As a final test of the influence of finite-size effects we repeated our calculations for an 18 site lattice at  $J/t=0.2$ . The result was in excellent agreement with Fig. 5(e).

Finally, we want to remark that some of the numerical results of this section have been obtained independently by Horsch *et al.*<sup>30</sup> However, in this work no attempt is made to explain the results based on the string picture developed above.

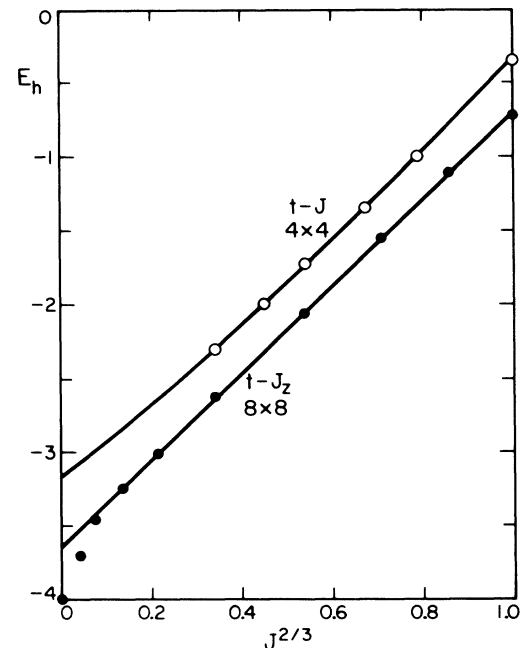


FIG. 13. Energy of the quasiparticle of the  $t$ - $J_z$  model with  $\mathbf{k}=(0,0)$  on a  $8\times 8$  lattice as a function of  $J_z^{2/3}$  showing its almost linear behavior (solid circles). For comparison we also show the energy of the quasiparticle in the  $t$ - $J$  model with  $\mathbf{k}=(\pi/2, \pi/2)$  on a  $4\times 4$  lattice versus  $J_z^{2/3}$  (open circles). The solid lines correspond to the best fit of the data discussed in the text. Since the best fit of the open circles is obtained with  $J^{0.73}$ , these points show some curvature.

### C. Bandwidth and spectral weight of the quasiparticle

How large is the effective mass of the hole? To answer this question we have measured the bandwidth ( $W$ ) of the dispersion relation  $E(\mathbf{k})$  of the quasiparticle. It is defined as the difference in energy between the maximum and minimum values of  $E(\mathbf{k})$ . This quantity gives us an indication about the effective mass of the hole once the effect of the nontrivial spin background is taken into account. It has been conjectured<sup>4</sup> that the effective mass is much bigger than the bare mass. This effect can be observed in small lattices ( $2 \times 2$ ) and also in relatively simple cases like 2 holes and one spin flip in an otherwise ferromagnetic background.<sup>17</sup> The reason is that the hole distorts the Néel spin background when it jumps from the even to the odd sublattices and that motion costs energy. A  $J$ - $t$ - $t'$  model where hopping in the same sublattice is allowed should present a smaller effective mass.

In the interval  $0.2 \leq J/t \leq 2.0$  (which contains the physically interesting region) we found numerically that the minimum (maximum) energy is produced by  $\mathbf{k}=(\pi/2, \pi/2)$  [ $\mathbf{k}=(0,0)$ ]. In Table V we present  $W$  versus  $J$  and in Fig. 14 we show  $\Delta\tilde{E}=E(\mathbf{k})-E(\pi/2, \pi/2)$  for many values of  $J/t$ . From Fig. 14 we can see that the bandwidth of the hole is highly anisotropic [then an analysis of the bandwidth will give us only indications about the effective mass in the  $a$ - $c$  direction in parameter space (Fig. 14)]. The qualitative behavior of  $\Delta\tilde{E}$  is basically the same in that broad range of parameter space. Its effective mass is much bigger along the direction  $b$ - $e$  than along  $a$ - $e$ . We also remark that care must be taken in Lanczos calculations of the bandwidth: We found that the state of lowest energy with  $\mathbf{k}=(0,0)$  has  $S=\frac{3}{2}$ , at least at  $J/t=0.2$ . This state should not be considered in the bandwidth since it belongs to a different band than the state with  $\mathbf{k}=(\pi/2, \pi/2)$ , which has  $S=\frac{1}{2}$ . Finally, in Fig. 15,  $W$  versus  $J$  is plotted. We think that the discontinuity at  $J/t \approx 2.0$  is due to a level crossing in the  $\mathbf{k}=(0,0)$  subspace (as it happens on a  $2 \times 2$  lattice). Note that for large  $J/t$  the bandwidth stays constant. This result will be explained in Sec. IV. Note that for

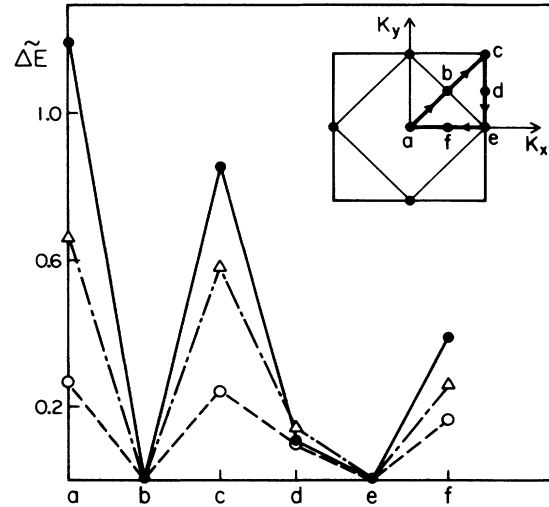


FIG. 14.  $\Delta\tilde{E}$  of the quasiparticle in the  $t$ - $J$  model (defined in the text) as a function of  $\mathbf{k}$  for  $J=0.2$  (open circles),  $J=0.4$  (triangles), and  $J=1.0$  (solid circles).

very small  $J/t$  the bandwidth seems to go negative. The reason is that the states with  $\mathbf{k}=(\pi/2, \pi/2)$  and  $\mathbf{k}=(0,0)$  cross in this region. We think this is just a finite-size effect as discussed before.

The data of Table V can be fit in two different ways. Based on the results of Ref. 4 we first attempted a fit  $W=a+bJ$ . Only for very small  $J/t$  we found this behavior. For example, for  $0.1 \leq J/t \leq 0.4$ ,  $W=-0.14+1.97J^{0.98}$  fits the data very well. This result is also in agreement with the calculations of Kane *et al.*<sup>4</sup> and the recent results of Trugman.<sup>31</sup> However, for higher values of  $J/t$  this fit is no longer good. Other functional forms have been tried in the literature<sup>42,43</sup> with better success. Another scenario is as follows. For  $0.1 \leq J/t \leq 0.4$  we found that the ground state in the  $\mathbf{k}=(0,0)$  subspace has an energy that can be fit reasonably well by  $-3.38+4.76J^{0.78}$ . Combining this result with the  $J$  dependence found above for the ground-state energy at  $\mathbf{k}=(\pi/2, \pi/2)$  (power-law  $J^{0.73}$ ), we conclude that the

TABLE V. Bandwidth ( $W$ ) of the quasiparticle in the  $t$ - $J$  model at different values of  $J$  (and  $t=1$ ) on a  $4 \times 4$  lattice.

$J$	$W$
0.20	0.271
0.30	0.478
0.40	0.667
0.55	0.894
0.70	1.038
1.00	1.194
1.25	1.293
1.50	1.395
1.75	1.507
2.00	1.630
2.50	1.532
3.00	1.456
5.00	1.262
10.00	1.189

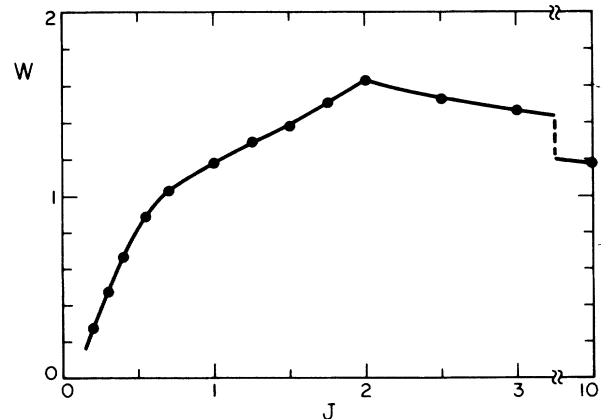


FIG. 15. Bandwidth ( $W$ ) of the quasiparticle of the  $t$ - $J$  model with  $\mathbf{k}=(\pi/2, \pi/2)$  on a  $4 \times 4$  lattice as a function of  $J$  ( $t=1$ ).

bandwidth may also have a power-law dependence with  $\alpha$  close to 0.7. If in the bulk limit the power-law dependence of both energies converges to the same number then that assumption is correct. Thus, we want to leave open such a possibility for the  $J$  dependence of  $W$ . Note that numerically this situation is difficult to analyze since using  $J^\alpha \approx J[1 + (\alpha - 1)\ln J]$  it is clear that for  $\alpha$  close to 1, an effective  $J^1$  law can be observed with logarithmic corrections. We also remark that in a recent paper<sup>44</sup> it has been claimed that  $W$  is a nonlinear function of  $J/t$ . This result was obtained using a new Green's function method.<sup>45</sup>

In Table VI we show the bandwidth for the  $t$ - $J_z$  model. As expected it is much smaller than for the  $t$ - $J$  model. The only source of coherent motion at small  $t/J$  are the high-order processes around the plaquettes described by Trugman<sup>8</sup> (see Sec. IV). Note, however, that for very small  $J_z/t$  ( $\approx 0.2$ ), the bandwidth of the  $t$ - $J_z$  and  $t$ - $J$  models are comparable.

We have also measured the spectral weight of the quasiparticle peak of Fig. 5. For large  $J/t$ , the calculation is not difficult since there is a well-defined peak at the bottom of the spectrum with few states close to it. However, reducing  $J/t$ , the density of states near the quasiparticle increases while its spectral weight decreases, and, to keep the same accuracy in that quantity as for large  $J/t$ , the peaks have to be separated reducing  $\epsilon$ . The resolution  $\Delta\omega$  of our numerical technique has to be reduced accordingly. The results are shown in Table VII. For  $J/t$  smaller than 0.1, the many crossing of levels near the ground state prevented us from extracting a reliable number. As with the bandwidth, the functional dependence of these results with  $J/t$  is not completely clear. For example, in the intermediate region  $0.2 \leq J/t \leq 1.0$  the data can be fit with a power-law  $J^\alpha$ , where  $\alpha$  is  $\approx 0.30$  but with a large error bar of 0.20. Note that a value around 1.0 seems to be excluded from our numerical data (Kane *et al.*<sup>4</sup> obtained  $\alpha=1$ ). However, if we reduce the interval in  $J/t$  to  $0.1 \leq J/t \leq 0.4$  then  $\alpha \approx 0.48 \pm 0.03$ , which is very close to the recent results of Trugman<sup>31</sup>  $\alpha=0.5$ . This is remarkable in view of the corresponding results for the bandwidth in the same interval (discussed above), where we also found excellent agreement with the results of Ref. 31. It is reasonable to conclude that the  $J$  dependence of the spectral weight seems well described by a power law which is smaller than 1 and close to 0.5 for small  $J/t$ .

For completeness, in Fig. 16 we show the density of

TABLE VI. Bandwidth ( $W$ ) of the quasiparticle in the  $t$ - $J_z$  model at different values of  $J_z$  (and  $t=1$ ) on a  $4 \times 4$  lattice.

$J_z$	$W$
0.0	0.299
0.2	0.210
0.4	0.113
0.7	0.055
1.0	0.029
2.0	0.004

TABLE VII. Spectral weight ( $S_W$ ) of the quasiparticle peak of Fig. 5 (in percentage of the total spectral weight) at many values of  $J$ .

$J$	$S_W$ (%)
0.10	20
0.20	28
0.30	35
0.40	40
0.55	46
0.70	51
1.00	59
3.00	84
5.00	91
10.00	96

states at  $J=0.2$ ,  $t=1$  obtained just by summing the spectral function over all momenta [ $D(\omega) = \sum_{\mathbf{k}} S(\mathbf{k}, \omega)$ ]. The different peaks found in Fig. 16 can be identified with a particular given momentum: I corresponds to  $\mathbf{k}=(\pi/2, \pi/2)$ ,  $\mathbf{k}=(\pi/2, 0)$ , and  $\mathbf{k}=(\pi/2, \pi)$ , and their rotated states; while peak II comes from  $\mathbf{k}=(0, 0)$ , and peak III from  $\mathbf{k}=(\pi, \pi)$ .

Finally note that it is also tempting to try to explain the structure observed in, for example, Fig. 5(e) as due to spin-wave excitations. We believe that this is not the correct language in the small  $J/t$  limit where the hole is delocalized and strongly affects the surrounding spins. In Table VIII we present the energy of the spin-wave excitations ( $S=1$ ) in the Heisenberg model (no holes). For  $J/t=0.2$  the energy required to create a spinwave of  $\mathbf{k}=(\pi, \pi)$  is too small to explain the structure found on top of the broadbands as due to these spin-waves. They can, however, explain the many small intensity peaks found in between the dominant peaks.

Summarizing this section, we found numerically that the ground state of one hole in the  $t$ - $J$  model has quasiparticle properties as predicted in Kane *et al.* However,

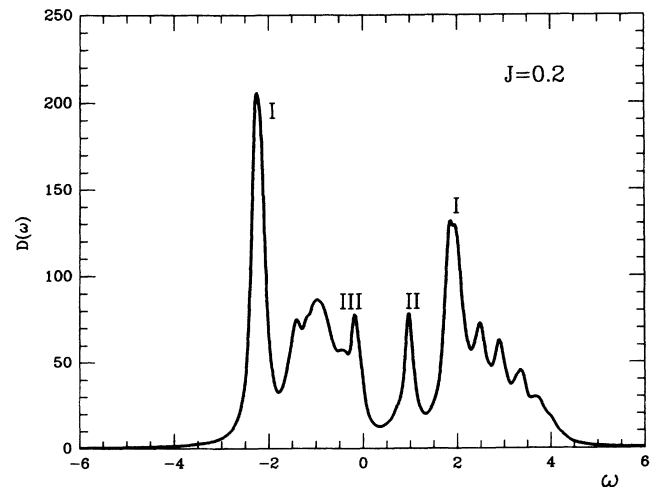


FIG. 16. Density of states of the  $t$ - $J$  model at  $J=0.2$  ( $t=1$ ) on a  $4 \times 4$  lattice. The labels I, II, and III of the peaks are explained in the text.

TABLE VIII. Energies of spin-waves excitations ( $S=1$ ) in the Heisenberg model for the  $4 \times 4$  lattice with different momenta  $\mathbf{k}$ .

$\mathbf{k}$	$E_{sw}$
(0,0)	1.711J
( $\pi, \pi$ )	0.578J
( $\pi/2, \pi/2$ )	2.710J
( $\pi, \pi/2$ )	2.342J
(0, $\pi/2$ )	2.434J

we did not find an incoherent band beyond the quasiparticle, but we found that the low-energy spectrum is well described by a string picture as in the Ising model. The bandwidth of the quasiparticle is greatly reduced and is roughly proportional to  $J$  at very small values of  $J$  (although a power-law behavior  $J^{0.7}$  similar to the ground state is not excluded). The spectral weight scales like  $J^{0.5}$  at small  $J/t$ . We think that the finite-size effects can be understood when deviations from this scaling are observed at small  $J$  and they do not affect strongly our analysis. It would be very interesting to compare our results Fig. 5 with photoemission experiments.<sup>46</sup> In particular it would be important to identify the string excitations beyond the quasiparticle.

#### IV. PERTURBATION THEORY IN THE LARGE $J/t$ LIMIT

##### A. Motivation

Our interest in this section is the regime  $J \geq t$  of the  $t$ - $J$  model, in which  $H$  is not related to the Hubbard model Hamiltonian. The investigation is not purely academic, however. This regime has the advantage that perturbation theory is valid, and certain features of the hole motion thereby become particularly clear. In particular, there are differences between the motion governed by the  $t$ - $J$  model [Eq. (1)] and motion governed by Ising-like modifications of Eq. (1) which we will discuss in detail. This is an important issue since many treatments of the  $t$ - $J$  model in the physically interesting regime  $J \leq t$  depend on expansions about some Néel-type state.<sup>3,4,5</sup>

We concentrate on the spin-liquid case, although comparison to states with long-range order are made. The superconducting state of the new high- $T_c$  materials lacks long-range spin order but retains a good deal of short-range order, so the liquid is the most interesting from the point of view of understanding superconductivity. We look only at one hole, therefore pairing itself is outside our scope. In addition, our numerical results are obtained on finite lattices; they can never have truly long-range order, although studies of susceptibilities can give good indications of the behavior of the ground state. Since we wish to compare our analytic results with numerical results, the liquid is of most interest to us. The present section is in contrast to most other treatments in this respect.

##### B. Structure of the perturbative calculation

We first consider the limit of very large  $J/t$ , say  $J/t > 20$ . The usual statement is that perturbation theory in  $t/J$  gives a bandwidth  $W$  proportional to  $t^2/J$ . Under what circumstances is this correct? To answer this question take a single hole in an antiferromagnet with  $t=0$ . The states of lowest energy may be written as  $c_{i,\sigma}|\psi_0\rangle$ , where  $|\psi_0\rangle$  is the ground state of the antiferromagnet with no holes. We are neglecting relaxation, which is not a large quantitative effect. Implicitly, we also ignore long-wavelength spin waves, a limitation which we discuss later.

The results will depend strongly on the choice of  $|\psi_0\rangle$ . The simplest possibility is that  $|\psi_0\rangle$  is the classical Néel state,  $|\psi_c\rangle$ , which would be the case if the transverse part of the spin-spin interaction were ignored. Then we find  $c_{i,\uparrow}|\psi_c\rangle=0$  if  $i$  belongs to the ‘down’ sublattice, and similarly  $c_{i,\downarrow}|\psi_c\rangle=0$  if  $i$  belongs to the ‘up’ sublattice. There are thus only  $N$  linearly independent states belonging to the low-energy subspace, where  $N$  is the number of sites. These states are all degenerate when  $t=0$ , so degenerate that perturbation theory is now required to find the band states. To first order, there are no matrix elements of the kinetic energy operator between the states. At second order, there are diagonal ‘self-energy’ contributions which shift the band but do not broaden it. Only at sixth order<sup>8</sup> does one find off-diagonal matrix elements so the states are split only by an amount  $\sim t^6/J^5$ . Hence the band is very narrow (in agreement with the numerical results of Sec. III). There are actually two bands in the reduced Brillouin zone, each corresponding to a definite spin and sublattice.

When we consider a nonclassical state  $|\psi_H\rangle$  with antiferromagnetic order, the situation becomes more complicated. Both  $c_{i,\uparrow}|\psi_H\rangle$  and  $c_{i,\downarrow}|\psi_H\rangle$  are nonzero, regardless of on which sublattice  $i$  sits. However, these two states have energies which differ by  $O(J)$ . Furthermore,  $c_{i,\uparrow}|\psi_H\rangle$  is degenerate with  $c_{j,\downarrow}|\psi_H\rangle$  when  $i$  and  $j$  belong to different sublattices. It is these states we must combine to make a band. In simple antiferromagnets, however, there is no perturbation matrix element coupling these states. The relevant quantity to calculate is  $\langle \psi_H | c_{i,\uparrow}^\dagger c_{i,\uparrow} c_{j,\uparrow}^\dagger c_{j,\downarrow} | \psi_H \rangle$ , where  $i$  and  $j$  are nearest neighbors. Using  $c_{\uparrow}^\dagger c_{\uparrow} = \frac{1}{2} + S^z$ ,  $c_{\downarrow}^\dagger c_{\downarrow} = \frac{1}{2} - S^z$ ,  $c_{\uparrow}^\dagger c_{\downarrow} = S^x + iS^y$ , and  $c_{\downarrow}^\dagger c_{\uparrow} = S^x - iS^y$ , we find this to be

$$\frac{1}{2} \langle \psi_H | S_j^x + iS_j^y | \psi_H \rangle + \langle \psi_H | S_i^z S_j^x + iS_i^z S_j^y | \psi_H \rangle .$$

This is zero in the Néel-ordered quantum states usually considered. In this case we find matrix elements only at second order between states  $c_{i,\sigma}|\psi_H\rangle$  and  $c_{j,\sigma}|\psi_H\rangle$ , where  $i$  and  $j$  are second or third neighbors. The bandwidth is therefore  $W_H \sim t^2/J$  at large  $J$ . On the other hand, the matrix element between nearest neighbors clearly does not vanish if there is spiral ordering of the spins. This choice of background spin state leads immediately to a bandwidth of order  $t$  at large  $J$ , which is the basis of the de Gennes canted states and also the more sophisticated spiral states of Shraiman and Siggia.<sup>21</sup>

In a spin-liquid state, call it  $|\psi_L\rangle$ , however, the struc-

ture of the perturbation theory becomes qualitatively different. Now the states  $c_{i,\uparrow}|\psi_L\rangle$ ,  $c_{i,\downarrow}|\psi_L\rangle$ ,  $c_{j,\uparrow}|\psi_L\rangle$ , and  $c_{j,\downarrow}|\psi_L\rangle$  ( $i$  and  $j$  on neighboring sites), are all degenerate. Most importantly, there is a *first-order* matrix element of the kinetic energy between  $c_{i,\uparrow}|\psi_L\rangle$  and  $c_{j,\uparrow}|\psi_L\rangle$ . Using the above operator identities we may easily calculate this matrix element:

$$\sum_{\sigma} \langle \psi_L | c_{i,\uparrow}^{\dagger} c_{i,\sigma} c_{j,\sigma}^{\dagger} c_{j,\uparrow} | \psi_L \rangle = \frac{1}{4} + \langle \psi_L | \mathbf{S}_i \cdot \mathbf{S}_j | \psi_L \rangle. \quad (11)$$

Note that this would reach its maximum value of  $\frac{1}{2}$  in a ferromagnet state and would be zero in a classical Néel state. Since  $\langle \psi_L | \mathbf{S}_i \cdot \mathbf{S}_j | \psi_L \rangle \approx -0.33$  for a low-energy liquid state,<sup>47</sup> we expect a bandwidth of  $W = -8t(\frac{1}{4} - 0.33) = 0.64t$ . Numerically, we found in Sec. III that, for the  $t$ - $J$  model and very large  $J/t$ , the bandwidth is approximately constant and equal to  $1.19t$ , while for the  $t$ - $J_z$  model it quickly vanishes increasing  $J_z$  [of course, we cannot show that this effect will survive the bulk limit without doing a finite-size scaling analysis (in preparation) but below we will *assume* that our numerical result is correct and discuss its consequences].

In a liquid state the bandwidth is proportional to  $t$  not  $t^2/J$ , when  $J \geq t$ . This conclusion refers to the position of the quasiparticle pole as  $\mathbf{k}$  changes and thus reflects a property of the coherent excitation. The weight in the quasiparticle pole is of order unity. In this limit, then, the quasiparticle act in a sense like a free particle with an effective mass  $m^*$  of roughly  $m^*/m_b \approx 10$  where  $m_b$  is the band mass.

To the extent that the conclusions hold at smaller  $J/t$  ratios, we see that spin liquids may well be favored at very modest hole concentrations. There is a large gain in kinetic energy per hole by going to the spin-liquid state for large  $J$ , whereas the loss in spin energy is comparatively small: The difference between the best energies for ordered states and liquid states is only a few percent but of course is proportional to  $J$ . At zero  $J$ , however, there is a *loss* of kinetic energy per hole in going to a liquid state. In the intermediate regime, however, it seems likely that only a rather small concentration of holes is needed to melt the antiferromagnet.

### C. Formal perturbation theory

In Sec. IV B, we discussed the structure of the large- $J$  limit, and, in particular, the qualitative consequences for the bandwidth. Here we look in detail at the perturbation calculation, concentrating on the case of liquid wave functions  $|\psi_L\rangle$ . The object is to calculate the full dispersion relation  $E(\mathbf{k})$  of the quasiparticles. We then compare with exact diagonalization studies. The liquid nature of the state means that we are working in the full Brillouin zone:  $-\pi < k_x \leq \pi$  and  $-\pi < k_y \leq \pi$ .

We have found that at very large  $J$ , the up eigenstates may be approximated as  $c_{\mathbf{R},\uparrow}|\psi\rangle$ , where  $|\psi\rangle$  is the ground state of the spin Hamiltonian and  $\mathbf{R}$  a lattice site. To do perturbation theory we need to find all up states which are connected to these states by one application of the kinetic-energy operator. The set of all such states is

$\sum_{\sigma} c_{\mathbf{R}+\hat{\delta},\sigma}^{\dagger} c_{\mathbf{R},\sigma}^{\dagger} c_{\mathbf{R},\sigma}$ . Therefore, we take as our basis states

$$\psi_{\mathbf{R},\uparrow} = \sqrt{2} \sum_{\sigma, \hat{\delta}} (a_{\hat{\delta}} c_{\mathbf{R}+\hat{\delta},\sigma}^{\dagger} c_{\mathbf{R},\sigma}^{\dagger} c_{\mathbf{R},\sigma} + a_0 c_{\mathbf{R},\uparrow}) |\psi\rangle, \quad (12)$$

where the  $a$ 's are coefficients to be determined. Here  $\hat{\delta}$  runs over the nearest neighbors and  $\mathbf{R}$  over all the sites. If  $|\psi\rangle$  is a singlet then  $\psi_{\mathbf{R},\uparrow}$  has spin  $\frac{1}{2}$ . The particular state here is a localized state which represents a hole exploring the 'well' formed by its neighbors. Note that  $\psi_{\mathbf{R},\uparrow}$  and  $\psi_{\mathbf{R}+\hat{\delta},\uparrow}$  are not orthogonal, but the overlap is again

$$\frac{1}{4} + \langle \psi | \mathbf{S}_{\mathbf{R}} \cdot \mathbf{S}_{\mathbf{R}+\hat{\delta}} | \psi \rangle \approx -0.08$$

for the spin-liquid state, so we ignore the corrections which come from this source, as is usual in the tight-binding theory that is isomorphic to the present formalism.

Translational invariance now demands that the eigenstates have the form

$$\begin{aligned} \psi_{\mathbf{k}} &= \frac{1}{\sqrt{N}} \sum_{\mathbf{R}} e^{i\mathbf{k} \cdot \mathbf{R}} \psi_{\mathbf{R},\uparrow} \\ &= \sqrt{2/N} \sum_{\sigma, \hat{\delta}, \mathbf{R}} [a_{\hat{\delta}}(\mathbf{k}) c_{\mathbf{R}+\hat{\delta},\sigma}^{\dagger} c_{\mathbf{R},\sigma}^{\dagger} c_{\mathbf{R},\sigma} + a_0(\mathbf{k}) c_{\mathbf{R},\uparrow}] |\psi\rangle. \end{aligned} \quad (13)$$

Hence for each  $\mathbf{k}$ , we only need to diagonalize a  $5 \times 5$  matrix to find the eigenvalues. The matrix is given by computing  $\langle \psi_{\mathbf{k}} | H | \psi_{\mathbf{k}} \rangle$  as a quadratic form in the  $a$ 's and taking the coefficients. The space in which we are working is a subspace of the variational space used by Trugman,<sup>8</sup> in the case where  $|\psi\rangle$  is an ordered antiferromagnet with spin-wave fluctuations.

To carry out this program, one needs to be able to calculate matrix elements of the form

$$\sum_{\sigma, \sigma'} \langle \psi | c_{\mathbf{R}+\hat{x}+\hat{y},\uparrow}^{\dagger} c_{\mathbf{R}+\hat{x}+\hat{y},\sigma'}^{\dagger} c_{\mathbf{R}+\hat{x},\sigma}^{\dagger} c_{\mathbf{R}+\hat{x},\sigma} c_{\mathbf{R},\sigma}^{\dagger} c_{\mathbf{R},\sigma} | \psi \rangle$$

which arise when the kinetic energy is evaluated between the states  $\psi_{\mathbf{R}+\hat{x}+\hat{y}}$  and  $\psi_{\mathbf{R}}$ . Such a term gives rise to an effective second-neighbor hopping and may be thought of as analogous to a Franck-Condon factor. It can be calculated using the operator identities of the last section with the result  $\frac{1}{2}(\frac{1}{4} + 2d_1 + d_2)$ , where we have introduced the notation  $d_n = \langle \psi | \mathbf{S}_i \cdot \mathbf{S}_j | \psi \rangle$ , where  $i$  and  $j$  are  $n$ th neighbors. This matrix element leads to a term in the quadratic form which may be expressed as

$$-\frac{t}{2} (\frac{1}{4} + 2d_1 + d_2) e^{i(k_x + k_y)} a_0 a_{\hat{x}} + \text{c.c.}$$

Other matrix elements may be evaluated similarly. More complicated matrix elements arise from the spin part of the Hamiltonian. The diagonal terms have the form

$$J \sum_{\langle i,j \rangle} \sum_{\sigma} \langle c_{\mathbf{R},\uparrow}^{\dagger} c_{\mathbf{R},\sigma}^{\dagger} c_{\mathbf{R}+\hat{\delta},\sigma}^{\dagger} \mathbf{S}_i \cdot \mathbf{S}_j c_{\mathbf{R}+\hat{\delta},\sigma} c_{\mathbf{R},\sigma}^{\dagger} c_{\mathbf{R},\uparrow} \rangle. \quad (14)$$

This is evaluated in the Appendix as

$$\frac{J}{2} \sum_{i,j \neq \mathbf{R}, \mathbf{R} + \hat{\delta}} \langle \mathbf{S}_i \cdot \mathbf{S}_j \rangle + \frac{J}{2} \sum_{i=\mathbf{R}, j \neq \mathbf{R} + \hat{\delta}} \langle \mathbf{S}_j \cdot \mathbf{S}_{\mathbf{R} + \hat{\delta}} - \mathbf{S}_j \cdot \mathbf{S}_{\mathbf{R}} \rangle + \frac{J}{2} \sum_{i \neq \mathbf{R} + \hat{\delta}, j=\mathbf{R}} \langle \mathbf{S}_i \cdot \mathbf{S}_{\mathbf{R} + \hat{\delta}} - \mathbf{S}_i \cdot \mathbf{S}_{\mathbf{R}} \rangle. \quad (15)$$

Referred to the zero of energy

$$\frac{J}{2} \sum_{i,j \neq \mathbf{R}} \langle \mathbf{S}_i \cdot \mathbf{S}_j \rangle$$

which is the spin energy with the vacancy, and using translational invariance, we find the diagonal elements  $\frac{1}{2}J(d_3 + 2d_2 - 3d_1)$ . Note that  $d_2 > 0$ ,  $d_3 > 0$ , and  $d_1 < 0$ , so this is a positive energy, consistent with the idea of the hole sitting in a potential well formed by the surrounding spin configuration. The matrix which now must be diagonalized is finally

$$\begin{pmatrix} \gamma_0 & -\gamma_x & -\gamma_y & -\gamma_{-x} & -\gamma_{-y} \\ -\gamma_x^* & \epsilon & 0 & 0 & 0 \\ -\gamma_y^* & 0 & \epsilon & 0 & 0 \\ -\gamma_{-x}^* & 0 & 0 & \epsilon & 0 \\ -\gamma_{-y}^* & 0 & 0 & 0 & \epsilon \end{pmatrix}. \quad (16)$$

correct to second order in  $t$ . The entries are defined as

$$E(\mathbf{k}) = -2\alpha_0 t (\cos k_x + \cos k_y) - 2(t^2/\alpha J) [(1 + 2\alpha_1 \cos k_x \cos k_y + \alpha_2 \cos 2k_x)^2 + (2\alpha_1 \sin k_x \cos k_y + \alpha_2 \sin 2k_x)^2 + (1 + 2\alpha_1 \cos k_y \cos k_x + \alpha_2 \cos k_y)^2 + (2\alpha_1 \sin k_y \cos k_x + \alpha_2 \sin 2k_y)^2]. \quad (20)$$

We take values of the correlation functions<sup>48</sup> as  $d_1 = -0.34$ ,  $d_2 = 0.20$ , and  $d_3 = 0.15$ , which gives  $\alpha_0 = -0.18$ ,  $\alpha_1 = -0.23$ ,  $\alpha_2 = -0.28$ , and  $\alpha = 1.58$ . Note that at very large  $J$ ,  $E(\mathbf{k})$  has its minimum at  $\mathbf{k} = (\pi, \pi)$  since in this case only the first term of  $E(\mathbf{k})$  counts and  $\alpha_0$  is negative. However, even at rather substantial values of  $J$ , the second term must be considered. For example, if we compare the energies  $E(\pi, \pi)$  and  $E(\pi/2, \pi/2)$ , we find that the latter becomes lower already at  $J/t \approx 7.5$ . This is in excellent qualitative agreement with the numerical results of Sec. III.

According to most analyses, the  $(\pi/2, \pi/2)$  state remains as the quasiparticle momentum of lowest energy down to small values of  $J$ . It is interesting that this is already found in large- $J$  perturbation theory. The origin of it lies in the fact that this state is able to propagate while at the same time maintaining the proper 'internal' phases, i.e., the symmetric wave function in the spin potential well. The  $(\pi, \pi)$  state, while propagating with the proper sign of the hopping matrix element from site to site, does not maintain the correct internal phase. In fact the coefficient of the  $t^2/J$  term nearly vanishes for this state. Thus there is a crossover from one state to the other at a surprisingly large value of  $J$ . Again, this is in agreement with our numerical results for the  $4 \times 4$  lattice.

#### D. Discussion

We conclude with some general remarks about our perturbative method. It is possible to do rigorous perturba-

$$\gamma_0/t = 2\alpha_0 (\cos k_x + \cos k_y),$$

$$-\gamma_x/t = 1 + 2\alpha_1 e^{ik_x} \cos k_y + \alpha_2 e^{2ik_x}, \quad \gamma_{-x} = \gamma_x^*, \quad (17)$$

$$-\gamma_y/t = 1 + 2\alpha_1 e^{ik_y} \cos k_x + \alpha_2 e^{2ik_y}, \quad \gamma_{-y} = \gamma_y^*,$$

and  $\epsilon = \alpha J$ . The constants  $\alpha_i$  are the only quantities which actually depend on the spin ground state. Their definitions follow from the discussion given above as

$$\alpha_0 = \frac{1}{2} + 2d_1, \quad \alpha_1 = \frac{1}{4} + 2d_1 + d_2, \quad (18)$$

$$\alpha_2 = \frac{1}{4} + 2d_1 + d_3, \quad \alpha = d_3 + 2d_2 - 3d_1.$$

The lowest eigenvalue is of most interest, as representing the quasiparticle dispersion. The other eigenvalues are associated with internal-excited states of the "polaron," or in other words, as a particle with differing number of magnons. The lowest eigenvalue correct to  $O(t^2)$  is

$$E(\mathbf{k}) = \gamma_0 - \sum_{\hat{\delta}=x,y} |\gamma_{\hat{\delta}}|^2 / \epsilon. \quad (19)$$

Fully written out, this is

tion theory once the zeroth-order basis states are chosen. These states should be eigenstates of the spin Hamiltonian which contain one hole. We chose the states  $c_{i\uparrow}|\psi\rangle$ , which are clearly not eigenstates since the spins surrounding the hole are not allowed to relax. The coordination of the sites around the site  $i$  is reduced and this increases the antiferromagnetic order on those sites.<sup>49,29</sup> This is clearly not taken into account in this wave function. However, this should make only small quantitative changes in the final results. We could write the real eigenfunction as  $R_i c_{i\uparrow}|\psi\rangle$ , where  $R_i$  is a "relaxation" operator, which converts the state into an eigenstate. The  $R_i$  and  $R_i^\dagger$  would then appear in the expressions which would determine the proper values of the coefficients  $\alpha$ . This should make only rather small quantitative changes in these parameters, and would not otherwise materially change the conclusions presented above.

A more serious approximation is the neglect of certain other states. For the perturbation theory to be valid, it is necessary to find all states which are connected by the kinetic-energy operator to the states in the low-energy subspace of the spin Hamiltonian. We restricted ourselves to states which could be reached by a single application, since this gives the largest matrix element. However, it is also possible to generate states by many applications of the kinetic term which might give a large contribution because they have small energy denominators. Physically, the most likely possibility of this kind are spin-wave states:  $c_{i\uparrow} a_q^\dagger |\psi\rangle$ , where  $a_q^\dagger$  creates a spin

wave. If  $\mathbf{q}$  is small [with respect to  $(\pi, \pi)$ ], then this state would have a low energy. The states actually used would correspond to linear combinations of the above with large  $\mathbf{q}$ , and therefore energy of order  $J$ . Thus our assumption is that at large  $J$ , the admixture of the small- $\mathbf{q}$  spin waves into the low-lying quasiparticle states is not too large, the idea being that spin-waves are high in energy for large enough  $J$ , and phase space at small  $\mathbf{q}$  is restricted. Finally, there is the *a posteriori* justification that the results qualitatively agree with the numerical results. The significance of this agreement is somewhat mitigated by the low- $\mathbf{q}$  cutoff present in any calculation on a finite lattice (more work is needed on the numerical side to convincingly show the existence of a spin-liquid state in the  $t$ - $J$  model).

Given that the perturbative picture is valid at large  $J$ , we may combine the results of Secs. I–IV to construct a comprehensive theory of the quasiparticle bandwidth. For very large  $J$ , there is a rigid quasiparticle which moves with bandwidth  $W=t$  in a liquid state or  $W=0$  in an antiferromagnetic state (at lowest order in  $t$ ). At moderately large  $J$  ( $\approx 5$ – $10t$ ), we get a polaron dominated by nearest-neighbors hops, i.e., its radius is one lattice constant.

There are corrections of order  $t^2/J$  to the bandwidth but with large coefficients. These corrections do not depend strongly on whether the hole moves in an antiferromagnetic background or a spin-liquid background. As  $J$  decreases further the polaron becomes larger and takes on a ‘string-like’ character, and the bandwidth crosses over at about  $J \approx t$  to a behavior  $J^{2/3}t^{1/3}$ , characteristic of a particle in a linear potential with slope  $\sim J$  and mass  $\sim 1/t$ . Thus the string is lengthening as  $J$  decreases. This picture persists until at least  $J \approx 0.1t$ . Again this regime is not expected to be very sensitive to whether the background state has long-range order or not. However, the string picture cannot continue to be valid at very small  $J$ . The string becomes very long and the time which the particle takes to explore the string, i.e., the inverse oscillation frequency in the linear potential, also becomes long; thus we expect the string to be erased. The spins will disorder and the well formed by the spin arrangement can no longer be regarded as a static ordered potential. We may give a quantitative criterion for the breakdown of the string picture in the following way. If the length of the string is  $L_s$  and the inverse oscillation frequency is  $T_s$ , then the string will be erased if  $\chi(L_s, T_s) \ll 1$ , where  $\chi$  is the dimensionless staggered susceptibility

$$\chi(\mathbf{r}, t) = e^{i\pi(x+y)/a} \langle S^z(\mathbf{r}, t) S^z(0, 0) \rangle, \quad (21)$$

where the expectation value is taken in the ground state of the spin system. Note that  $L_s \sim J^{-1/6}$  and  $T_s \sim J^{-1/6}$ , and  $\chi(\mathbf{r}, t)$  is a decreasing function of both  $|\mathbf{r}|$  and  $t$ . The small exponent explains the fact that the small- $J$  regime is not reached at  $J \sim 0.1t$ , as might naively be expected. Note also that the string will be more robust in an ordered spin background, where the falloff of  $\chi$  with  $|\mathbf{r}|$  is presumably slower. At very small  $J$  it is likely that the bandwidth is proportional to  $J$ . We conclude that the string picture has a remarkably wide range of validity.

## V. HUBBARD MODEL WITH ONE HOLE: DYNAMICAL PROPERTIES

In addition to the  $t$ - $J$  model we have also studied numerically the one-band Hubbard model defined by the Hamiltonian,

$$H = -t \sum_{i, \delta, \sigma} (c_{i, \sigma}^\dagger c_{i+\delta, \sigma} + \text{H.c.}) + U \sum_i (n_{i, \uparrow} - \frac{1}{2})(n_{i, \downarrow} - \frac{1}{2}), \quad (22)$$

where the notation is standard. In particular, we analyzed ground-state energies in the ‘‘0 and 1 hole’’ subspaces (defined as the half-filled and one-electron-less-than half-filled subspaces, respectively) and the spectral function of one hole. The energy of the ground state in the subspace with total spin one ( $S=1$ ) and zero holes (that becomes the ‘‘spin-wave’’ state at large  $U/t$ ) was also studied. We used lattices with 8 and 10 sites arranged as shown in Fig. 17 (they have the same symmetries under rotations as the bulk lattice). The allowed momenta are  $\mathbf{k} = (\pm\pi/2, \pm\pi/2)$ ,  $(0, \pi)$ ,  $(\pi, 0)$ ,  $(0, 0)$ , and  $(\pi, \pi)$  for the 8 site lattice, and  $\mathbf{k} = (3\pi/5, \pi/5)$ ,  $\mathbf{k} = (2\pi/5, 4\pi/5)$  (plus their  $\pi/2$  rotated states), and  $(0, 0)$ ,  $(\pi, \pi)$  for the 10 site lattice. Since the size of the Hilbert space of this model grows faster with the number of sites than in the  $t$ - $J$  model, a study of the 16 site lattice would have required considerably more work, and thus we restricted our analysis to these small clusters.

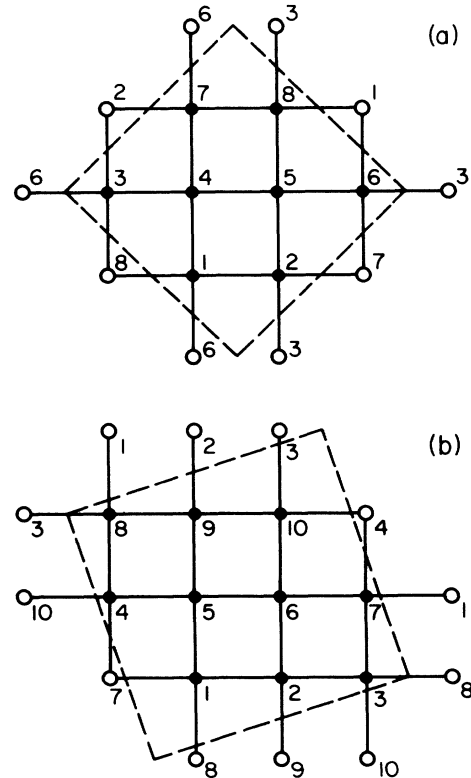


FIG. 17. Geometry of the 8 and 10 site lattices used for the Hubbard model. Solid circles are the sites of the lattice while open circles denote the neighbors.

TABLE IX. Ground-state energy of the Hubbard model with 0 and 1 holes as a function of  $U$  (at  $t=1$ ). The difference in energies is the hole energy ( $E_h$ ). Results are presented for the 8 and 10 site lattices.

$U$	8 sites			10 sites		
	0 hole ( $S=0$ )	1 hole ( $S=\frac{1}{2}$ )	$E_h$	0 hole ( $S=0$ )	1 hole ( $S=\frac{1}{2}$ )	$E_h$
0	-8.0000	-8.0000	0.0000	-16.0000	-15.0000	1.0000
1	-9.1826	-8.8084	0.3742	-16.1541	-15.1369	1.0172
2	-10.4721	-9.7217	0.7505	-16.6113	-15.5451	1.0662
4	-13.3202	-11.8007	1.5195	-18.4075	-17.1305	1.2770
8	-19.7840	-16.6446	3.1394	-25.1041	-22.5679	2.5362
10	-23.2687	-19.2798	3.9889	-29.2821	-25.8991	3.3830
20	-41.8775	-33.3583	8.5192	-52.3517	-44.4490	7.9027
40	-80.9831	-62.8104	18.1727	-101.2150	-83.7423	17.4727

Only two technical details should be mentioned here besides those discussed before for the  $t$ - $J$  model. In the Hubbard model it is important to use the fermionic representation for the electrons explicitly. Even for the 0 and 1 hole subspaces electron-hole pairs (charge fluctuations) can be created and destroyed and effectively we are dealing with a multi-fermion problem. As remarked before (Sec. III), there is a shift of  $(\pi, \pi)$  in the momentum of the ground state of the  $t$ - $J$  model between the fermionic and bosonic representations. States with  $\mathbf{k}=(\pi, \pi)$  in the Hubbard model should be compared with states with  $\mathbf{k}=(0, 0)$  in the  $t$ - $J$  model (for more details see Ref. 38). The other technical point concerns the numerical technique: If the iterations of the modified Lanczos method start with a state having a definite momentum and  $S^z$ , but no definite total spin, then for the 8 site lattice we observed a severe slowing down in the convergence due to the existence of states with  $S=\frac{3}{2}$  and  $S=\frac{1}{2}$  very close in energy to each other at the bottom of the one-hole spectrum (as discussed later). This problem is solved by using an initial configuration with definite spin. We also found it very convenient to work with increasing  $U/t$  using as starting configuration the exact ground state of the previously analyzed value of  $U/t$ . Using this trick with just  $\approx 10$ -15 iterations the energy was obtained with error  $10^{-9}$  for many values of  $U/t$ .

In Table IX we present the ground-state energies of the model with 0 and 1 holes (and *minimum* spin) and its difference defined as the energy of a hole ( $E_h$ ). In the absence of holes the ground state is a singlet  $S=0$  and its

TABLE X. Energy of the ground state in the subspace with one hole and  $S=\frac{3}{2}$ , with respect to the ground-state energy with one hole and  $S=\frac{1}{2}$ . Results are presented for the 8 and 10 site lattices, at  $t=1$ .

$U$	$\Delta E_{3/2}$	$\Delta E_{3/2}$
	(8 sites)	(10 sites)
0	0.0000	2.000
1	-0.0032	1.624
2	-0.0128	1.291
4	-0.0568	0.798
10	-0.2889	0.274
20	-0.5454	0.095
40	-0.7268	0.013

total momentum is  $\mathbf{k}=(0, 0)$ . For one hole, the lowest energy state with  $S=\frac{1}{2}$  has a nonzero momentum for a wide range of values of  $U/t$ . In particular, for the 8 site lattice that momentum is  $\mathbf{k}=(\pi/2, \pi/2)$  [which is degenerate with  $\mathbf{k}=(\pi, 0), (0, \pi)$  due to the special geometry of this lattice as happens with the  $4 \times 4$  lattice for both the  $t$ - $J$  and Hubbard models with nearest-neighbors interactions]. For the 10 site lattice the momentum of the hole is  $\mathbf{k}=(3\pi/5, \pi/5)$  (plus rotated states) which does not have spurious degeneracies. These momenta belong to the Fermi surface of the model at  $U/t=0$ . A similar situation was reported for the  $t$ - $J$  model with 10 and 16 sites.<sup>9,29</sup>

In Table X we also show the difference between the ground-state energies for one hole with total spin  $S=\frac{3}{2}$  and  $S=\frac{1}{2}$ . For the 8 site lattice we found the surprising result that this gap is negative (the state with  $S=\frac{3}{2}$  is the actual ground state) for a broad range of values of  $U/t$  including weak coupling (showing that this result is unrelated with the ferromagnetism expected at large  $U/t$  due to Nagaoka's theorem). This effect was previously observed for one value of  $U/t$  in Ref. 50. For very large  $U/t$ , higher spin states become the ground state and there is a transition to the Nagaoka phase. For the 10 site lattice and for the  $t$ - $J$  model we have not observed the same effect. Note that for the 10 sites Hubbard model there is a gap between the states with  $S=\frac{1}{2}$  and  $S=\frac{3}{2}$  at  $U/t=0$ , while for a 16 sites Hubbard model they are degenerate at that value of  $U/t$  and perhaps both states will again be close in energy as for the 8 site lattice. Below, we will continue our study of bandwidths and other quasiparticle properties working in the  $S=\frac{1}{2}$  subspace rather than for  $S=\frac{3}{2}$ , i.e., we will assume that the result described above concerning the  $S=\frac{3}{2}$  spin of the ground state of one hole in the 8 site lattice is a finite-size effect (perhaps perturbation theory can be applied to study the spin of the ground state with one hole to clarify this point in the bulk limit).

In Figs. 18 and 19 we show the density of states of one particle in the one-band Hubbard model for different values of  $U/t$  and for the 8 and 10 site lattices, respectively. The definition of  $D(\omega)$  and the technique used are the same as for the  $t$ - $J$  model (Sec. III). The particle-hole symmetry of the Hamiltonian Eq. (22) is the origin of the reflexion symmetry  $\omega \rightarrow -\omega$  of Figs. 18 and 19. For the 8 site lattice the peaks I of Fig. 18(c) correspond

to  $\mathbf{k}=(\pm\pi/2,\pm\pi/2)$  and  $\mathbf{k}=(\pi,0), (0,\pi)$ . Peak II corresponds to  $\mathbf{k}=(0,0)$ , while peak III denotes  $\mathbf{k}=(\pi,\pi)$ . For the 10 site lattice, in Fig. 19(c) the meaning of peaks II and III is the same while peak I correspond to  $\mathbf{k}=(3\pi/5,\pi/5)$  and peak IV to  $\mathbf{k}=(2\pi/2,4\pi/5)$  (plus their rotated states).

Note that for both lattices there is a sharp peak at the bottom of the  $\omega>0$  band signaling the existence of a quasiparticle as in the  $t$ - $J$  model. As expected, the gap in the one-particle sector increases with  $U/t$  and there are no indications in these small lattices of a critical  $U/t$  separating metallic from insulating regimes. Thus, this model seems to have insulating properties for all values of  $U/t\neq 0$ . Perhaps adding next-nearest neighbors interactions a finite critical  $U/t$  can be induced. Note also that the smooth connection found between strong and weak coupling gives more support to theories of superconductivity that begin the analysis of the model in perturbation

theory rather than in strong coupling as suggested experimentally. There seems to exist an analytic connection between both regimes. It is also interesting to remark that Figs. 18 and 19 are very similar and, thus, the finite-size effects do not appear to be very severe in our analysis.

From Figs. 18 and 19 we observe that for these small lattices the density of states does not have much structure. In weak coupling this can be understood easily since the state  $|1\rangle$  used in the spectral function (see Sec. III) is an eigenstate of the model at  $U/t=0$  and thus each  $S(\mathbf{k},\omega)$  presents only one peak. For  $U/t\neq 0$  there are more peaks than those that can be distinguished in Figs. 18 and 19 but they have very small spectral weight. Perhaps increasing the size of the lattice other states with large spectral weight may appear. In particular, for large  $U/t$  and a  $4\times 4$  lattice we should recover the results presented before for the  $t$ - $J$  model.

We found that the analysis of the bandwidth of the

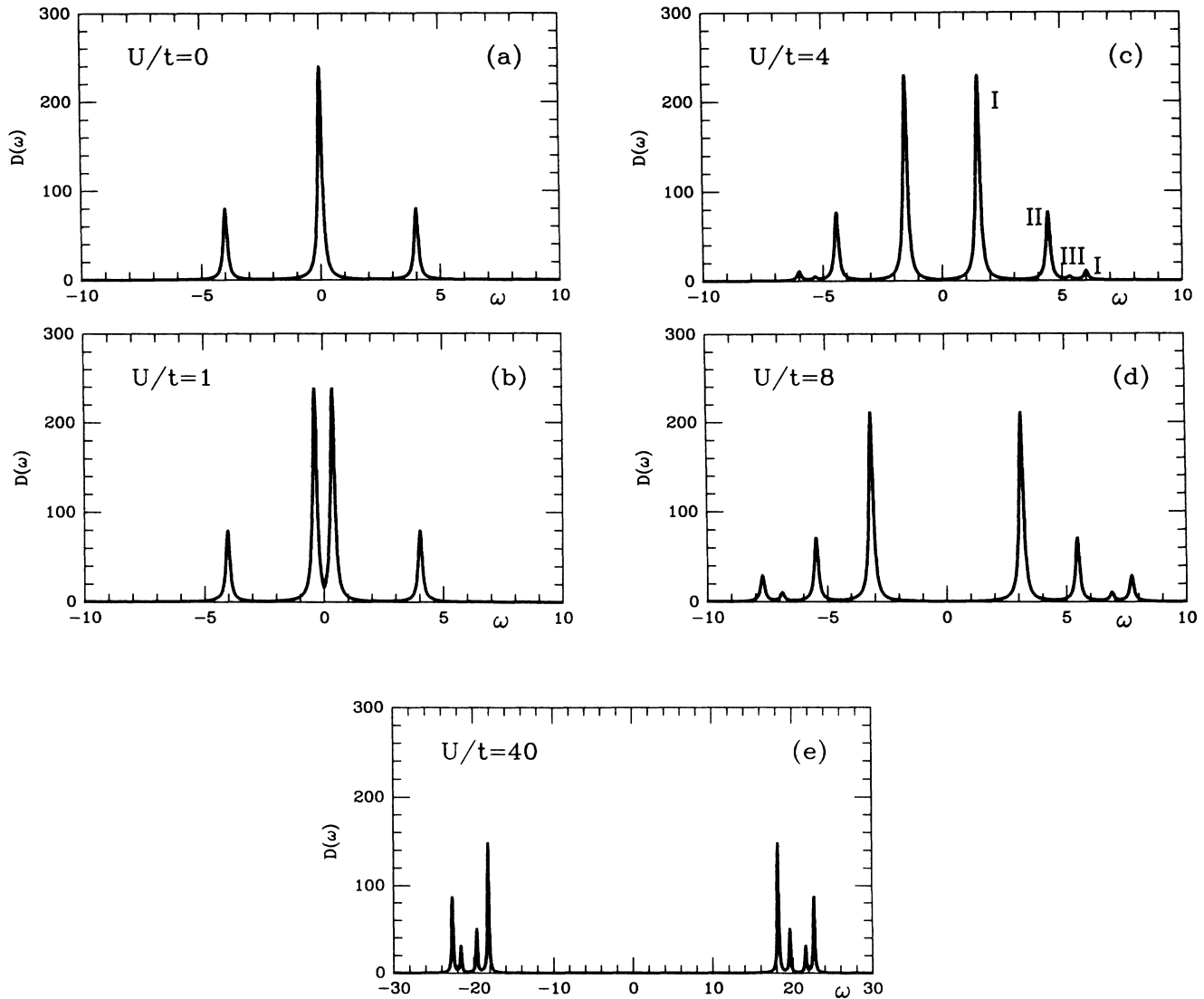


FIG. 18. Density of states  $[D(\omega)]$  of the Hubbard model on an 8 site lattice for many values of  $U/t$ : (a)  $U/t=0$ ; (b)  $U/t=1$ ; (c)  $U/t=4$ ; (d)  $U/t=8$ ; (e)  $U/t=40$ . The meaning of peaks I, II, and III of (c) is explained in the text (we used  $\varepsilon=0.1$  in this figure and 80 iterations of the continuous fraction expansion were performed).

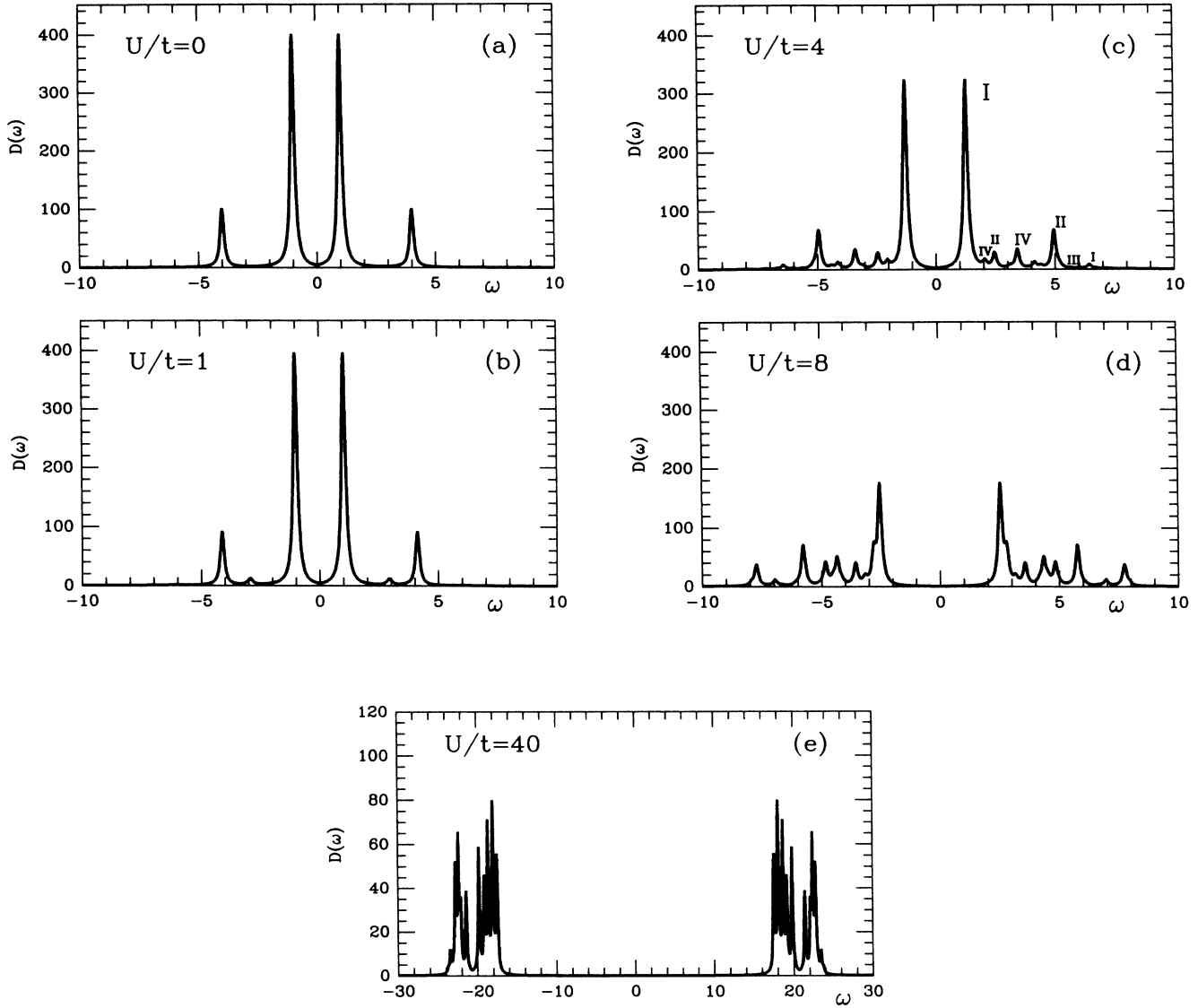


FIG. 19. Density of states [ $D(\omega)$ ] of the Hubbard model on a 10 site lattice for many values of  $U/t$ : (a)  $U/t=0$ ; (b)  $U/t=1$ ; (c)  $U/t=4$ ; (d)  $U/t=8$ ; (e)  $U/t=40$ . The meaning of peaks I, II, III, and IV of (c) is explained in the text (we used  $\varepsilon=0.1$  in this figure and 80 iterations of the continuous fraction expansion were performed).

quasiparticle in the Hubbard model is difficult. In Table XI we show the numerical values for the bandwidth ( $W$ ) defined, as for the  $t$ - $J$  model, as

$$W = \max[E(\mathbf{k})] - \min[E(\mathbf{k})],$$

where  $E(\mathbf{k})$  is the dispersion relation of the quasiparticle in the  $S=\frac{1}{2}$  sector. For the 8 site lattice we found that the minimum in energy occurs at  $\mathbf{k}=(\pi/2, \pi/2)$  [degenerate with  $\mathbf{k}=(\pi, 0), (0, \pi)$ ] and the maximum at  $\mathbf{k}=(\pi, \pi)$ . For 10 sites the minimum is at  $\mathbf{k}=(3\pi/5, \pi/5)$  and the maximum also at  $\mathbf{k}=(\pi, \pi)$ . This situation occurs for a wide range of values of  $U/t$  [the small spectral weight of the state with  $\mathbf{k}=(\pi, \pi)$  is a

TABLE XI. Bandwidth ( $W$ ) of the Hubbard model for the 8 and 10 site lattices at  $t=1$ .

$U$	$W$ (8 sites)	$W$ (10 sites)
1	3.9033	3.6178
2	3.8487	3.2031
4	3.8007	2.5323
6	3.7747	2.1073
8	3.7457	1.8359
10	3.7121	1.6377
20	3.5604	1.0307
40	3.4197	0.6877

simple consequence of the physics of the noninteracting limit  $U/t=0$ , where the zero-hole ground state has no populated one-particle states with that momentum]. The problem in extracting useful information from Table XI is the large difference between the 8 and 10 sites results. While at small  $U/t$  that difference can be understood from the particular values of the energy states of the noninteracting problem, the large difference at large  $U/t$  is puzzling. We observed that the one-hole energy at the bottom of the quasiparticle band at  $U/t=20$ , for example, differs in only 7% between the two lattices while at the maximum of the band the difference is 26%. Then, as in the  $t$ - $J$  model, we have found that a numerical calculation of the bandwidth is very difficult due to the erratic behavior of the higher energy states of the quasiparticle band. We insist that the important physical quantity is not  $W$  but the mass at the bottom of the band which is, however, difficult to calculate on a small lattice. Note also that  $W$  at  $U/t=20$  for both lattices is appreciably bigger than the bandwidth for the  $t$ - $J$  model on a 16 site lattice at  $J=0.2$ . This may be a finite-size effect (we are comparing different lattice sizes) or it may be due to the absence of hopping terms in the  $t$ - $J$  model between sites on the same sublattice. Those terms are not explicit in the Hubbard model but are generated in its strong coupling effective Hamiltonian. It is clear that in the presence of intrasublattice hopping terms the holes are more mobile and its effective mass is smaller increasing the bandwidth. A study of the  $J$ - $t'$  model (in preparation) may answer this question.

In the Hubbard model we have the same problem as for the  $t$ - $J$  model to distinguish between the energies of the hole states with  $\mathbf{k}=(\pi/2, \pi/2)$  or  $\mathbf{k}=(\pi, 0), (0, \pi)$  in the bulk limit. For the 10 site lattice the splitting between the states nearest to those two, i.e.,  $\mathbf{k}=(3\pi/5, \pi/5)$  and  $\mathbf{k}=(2\pi/5, 4\pi/5)$  is very small (at large  $U/t$ ) showing that to answer this question properly bigger lattices are needed.

It is very interesting to compare our density of states shown in Figs. 18 and 19 with the results obtained in a recent Monte Carlo simulation,<sup>51</sup> where a new numerical method to extract real time properties from imaginary time results was presented. In Fig. 20 we put together

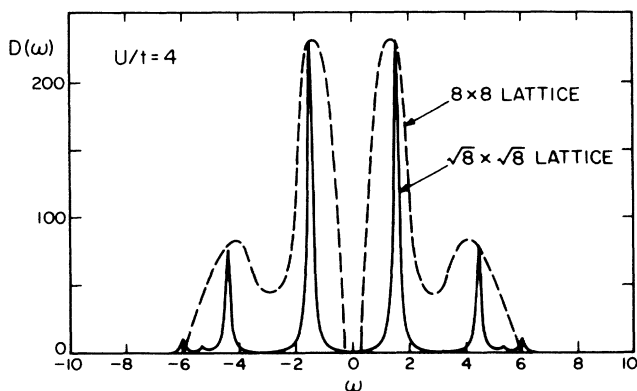


FIG. 20. Comparison of our density of states Fig. 18(c) for an 8 site lattice (continuous line) with the Monte Carlo results of Ref. 51 (dashed line).

Fig. 3 of Ref. 51 and our Fig. 18(c), corresponding to the density of states of the Hubbard model at  $U/t=4$ . The Monte Carlo result was obtained using a  $8 \times 8$  lattice and working at small temperature while the exact result corresponds to the 8 site lattice. Since the weight of the peaks can be changed with  $\epsilon$  we plot both graphs following the convention that the maximum value of  $D(\omega)$  is the same for both cases. It is clear that the agreement between both methods is very good not only at low energies but also at intermediate energies  $\omega \approx 4$ . Then, the second broad bump observed in the Monte Carlo simulation is real and due to the contribution of the sector with zero momentum [peak II of Fig. 18(c)].

It is very interesting that, with respect to dynamical quantities, it is possible to obtain the same information that present day Monte Carlo techniques provide just by using a small lattice and exact diagonalization techniques. Both techniques should be used in a complementary way. The Monte Carlo method allows us to study large lattices but with low resolution in  $\omega$  and at finite temperature while the Lanczos method is exact but restricted to small lattices. For large values of  $U/t$  and arbitrary doping fraction where Monte Carlo methods are difficult to apply, the Lanczos method is our only reliable technique. A good agreement between the Monte Carlo and Lanczos methods has also been found in the individual spectral functions. For  $\mathbf{k}=(\pi/2, \pi/2)$  it was observed<sup>51</sup> that at  $U/t=4$  and 2 a small peak appears at  $\omega \approx 4$  besides the large peak at small  $\omega$ . We think that this second peak is related to the additional structure that we found in the spectral function at that momentum on the 8 site lattice at  $\omega \approx 6$ . Although we do not have a proof, we conjecture that this second peak can also be associated with the broad second band observed for the first time in Ref. 29 in the spectral function of the  $t$ - $J$  model [see for example Fig. 5(e)]. In the limit of large  $J$  in the  $t$ - $J$  model, that peak corresponds to a “string” excitation of length one as that shown in Fig. 10. Then, we believe that the second bump observed in the Monte Carlo simulation corresponds to a higher energy state of the string picture described in detail in Sec. III.

In Table XII we show the energy (relative to the half-filled ground state) of the first state with  $S=1$  and  $\mathbf{k}=(\pi, \pi)$  that we call the spin-wave state. For small  $U/t$  there is a large difference in energy between the 8 and 10 site lattices due to the absence of a zero-energy one-particle state at  $U/t=0$  for the latter. For large  $U/t$  the agreement is better. It is important to compare this result with the corresponding spin-wave gap of the Heisenberg model. We have obtained that gap numerically and it is  $J$  and  $0.836J$  for the 8 and 10 site lattice Heisenberg model, respectively. Then at  $U=40$  ( $t=1$ ) or equivalently  $J=0.1$ , those energies are 0.10 and 0.0836 to be compared with 0.093 and 0.079, respectively, for the Hubbard model (Table XII). Only a rough agreement (around 7%) is found even for this large value of  $U/t$  showing that the  $t$ - $J$  and Hubbard models only agree quantitatively at very large  $U$  (although qualitatively they are very similar in a wider range). The comparison quickly deteriorates on reducing  $U/t$  (perhaps keeping more terms in the effective Hamiltonian derived from the

TABLE XII. Energy of the “spin wave” state ( $E^{\text{SW}}$ ) with respect to the ground state of 0 hole for the 8 and 10 site lattices (at  $t=1$ ).

$U$	$E^{\text{SW}}$ (8 sites)	$E^{\text{SW}}$ (10 sites)
0	0.0000	2.0000
1	0.0072	1.6116
2	0.0258	1.2540
4	0.0776	0.6639
6	0.1247	0.3414
8	0.1555	0.2408
10	0.1709	0.2070
20	0.1531	0.1394
40	0.0931	0.0794

Hubbard model in strong coupling we may get a better agreement). In particular, note that the spin-wave energy for the 8 site lattice has a maximum at intermediate values of  $U/t$  and then goes to zero in the noninteracting limit (a similar situation should occur on a 16 site lattice). Then, it is quite possible that in the region where attraction of holes was found in the Hubbard model<sup>25</sup> (Fig. 2), the  $t$ - $J$  and Hubbard models are quantitatively very different as conjectured before. To give additional support to this claim in Fig. 21 we show the 24 energy levels (many of them degenerate) of the Hubbard model with one hole on a  $2 \times 2$  lattice with  $S_z = \frac{1}{2}$  which can be solved exactly. We clearly observe that the states containing doubly occupied sites pay high energies at large  $U/t$  and eventually decouple from the rest. At least in this tiny lattice the separation of the two bands is very large only at very small  $J=4t^2/U$ . For example, at  $U/t=4$  ( $J=1$  in the  $t$ - $J$  model) replacing the Hubbard model by the  $t$ - $J$  model or any other strong-coupling effective Hamiltonian with only three states per site is clearly wrong since the two bands are strongly mixed. Actually, from Fig. 21 we can conclude that the radius of

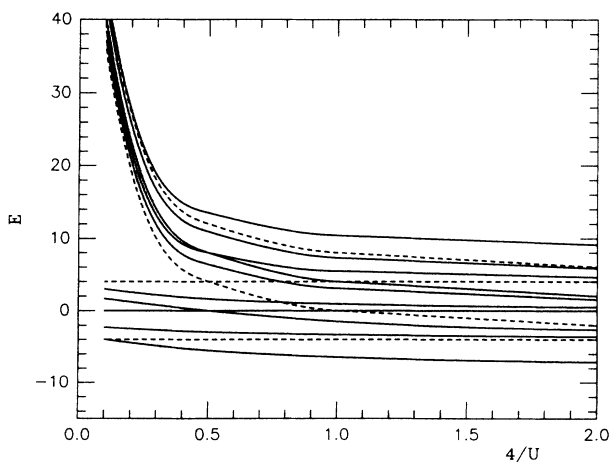


FIG. 21. Evolution of the energy levels of the Hubbard model with one hole on a  $2 \times 2$  lattice solved exactly.  $t$  was taken equal to 1 and thus  $4/U$  is equal to  $J$  of the  $t$ - $J$  model. The solid (dashed) lines denote degenerate (nondegenerate) states. The ground state has  $\mathbf{k}=(0, \pi)$  and  $(\pi, 0)$ .

convergence of the strong-coupling expansion of the Hubbard model lies at around  $J \approx 0.5$ . This is in excellent agreement with all our conclusions above regarding a comparison between the Hubbard and  $t$ - $J$  models.

## VI. CONCLUSIONS

In this paper we have studied the behavior of one hole in the  $t$ - $J$  and one band Hubbard models. The analysis was done using Lanczos techniques on small lattices and perturbation theory at large  $J/t$  in the bulk limit. In particular, we present the first numerical results for the one-hole spectral function of strongly correlated electronic models. In the  $t$ - $J$  model we found a large peak at the bottom of that spectral function that we associate with a quasiparticle. For small  $J/t$  the position of that peak (energy of the hole) is well reproduced by  $E_h = -3.17 + 2.83J^{0.73}$  (for  $0.1 \leq J \leq 1.0$ ). The rest of the spectrum is not incoherent but presents structure. In particular, there are at least two additional peaks following a similar power law while at large energies a pseudogap separates the first band from a second broad band. We argue that the low-energy behavior can be understood by describing the hole as a particle in a confining linear potential as it happens in the Ising limit. This result is far from obvious since it was assumed that the spin fluctuations of the Heisenberg model would erase that string. We show that this is not true at least for the low-energy sector. Of course, it would be very important to verify our conclusions by numerically working on larger lattices.

The bandwidth of the hole was also evaluated. At small  $J/t$  it is linear in  $J$  (although a power law  $J^{0.7}$  is not excluded) while at large  $J/t$  it is proportional to  $t$ . This last result can be understood from perturbation theory in  $t/J$  assuming that the ground state has spin liquid characteristics rather than long-range antiferromagnetism. The spectral function of the hole was also presented: At small  $J/t$  it behaves as  $J^{0.5}$ . We compared all these results with the  $t$ - $J_z$  Ising model.

The one-hole spectral function of the one-band Hubbard model was obtained on 8 and 10 site lattices. A quasiparticle was found at the bottom of the spectrum. We show that our Lanczos results provide similar information as that given by recent Monte Carlo simulations on larger lattices. We also compared our results for this model with the  $t$ - $J$  model concluding that they agree quantitatively only at very small  $J/t$  (large  $U/t$ ).

## ACKNOWLEDGMENTS

This project was supported in part by the National Science Foundation (NSF) Grant Nos. PHY87-01775, PHY82-17853, DMR-88128852, and DMR-8612860, the Electric Power Research Institute, and by the Department of Energy Grant No. FG03-88-ER45197 at the University of California, Santa Barbara and supplemented by funds from U. S. National Aeronautics and Space Administration (NASA). The computer simulations were done on the CRAY-2 at National Center for Supercomputing Applications (NCSA), University of Illinois at Urbana-Champaign. We thank NCSA for their support.

## APPENDIX

We wish to evaluate the matrix element

$$M = \sum_{(i,j)} \sum_{\sigma,\sigma'} \langle c_{\mathbf{R},\uparrow}^\dagger c_{\mathbf{R},\sigma} c_{\mathbf{R}+\hat{\delta},\sigma}^\dagger \mathbf{S}_i \cdot \mathbf{S}_j c_{\mathbf{R}+\hat{\delta},\sigma'} c_{\mathbf{R},\sigma}^\dagger \rangle. \quad (\text{A1})$$

Here  $i$  and  $j$  are nearest neighbors and  $\hat{\delta}$  is a nearest-neighbor vector. In a liquid we may rewrite this as

$$2M = \sum \langle c_{\mathbf{R},\uparrow}^\dagger c_{\mathbf{R},\sigma'} c_{\mathbf{R}+\hat{\delta},\sigma''}^\dagger \mathbf{S}_i \cdot \mathbf{S}_j c_{\mathbf{R}+\hat{\delta},\sigma''} c_{\mathbf{R},\sigma}^\dagger \rangle. \quad (\text{A2})$$

A summation with no indices is over  $i, j, \sigma, \sigma', \sigma''$ . There are three separate cases to consider.

(i)  $i \neq \mathbf{R}, i \neq \mathbf{R} + \hat{\delta}, j \neq \mathbf{R}, j \neq \mathbf{R} + \hat{\delta}$ . Now the creation and annihilation operators commute with the spin operators. Thus  $M$  may be written as

$$2M = \frac{1}{2} \sum \langle \mathbf{S}_i \cdot \mathbf{S}_j c_{\mathbf{R},\sigma}^\dagger c_{\mathbf{R},\sigma'} c_{\mathbf{R}+\hat{\delta},\sigma''}^\dagger c_{\mathbf{R}+\hat{\delta},\sigma'''} c_{\mathbf{R},\sigma}^\dagger \rangle. \quad (\text{A3})$$

Moving  $c_{\mathbf{R},\sigma'}$  to the right and noting that  $\langle c_{\mathbf{R},\sigma} c_{\mathbf{R},\sigma} \rangle = 0$  for any spin state, this term is seen to be

$$M = \frac{1}{2} \sum \langle \mathbf{S}_i \cdot \mathbf{S}_j c_{\mathbf{R}+\hat{\delta},\sigma'}^\dagger c_{\mathbf{R}+\hat{\delta},\sigma''}^\dagger c_{\mathbf{R},\sigma}^\dagger \delta_{\sigma',\sigma''} c_{\mathbf{R},\sigma} \rangle = \frac{1}{2} \sum_{i,j} \langle \mathbf{S}_i \cdot \mathbf{S}_j n_{\mathbf{R}+\hat{\delta}} n_{\mathbf{R}} \rangle = \frac{1}{2} \sum_{i,j} \langle \mathbf{S}_i \cdot \mathbf{S}_j \rangle. \quad (\text{A4})$$

This simply reflects the fact that if the added hole does not visit some pair of sites, then their bond is undisturbed by its motion.

(ii)  $j = \mathbf{R} + \hat{\delta}$ . In this case we rewrite  $\mathbf{S}_j$  as  $c_{j,\sigma}^\dagger \sigma_{\sigma,\sigma'} c_{j,\sigma'}$  and move the pair  $c_{j,\sigma'} c_{\mathbf{R}+\hat{\delta},\sigma''}$  to the right, where it annihilates the spin state. Hence  $M=0$  for this case. The same statement holds for  $i = \mathbf{R} + \hat{\delta}$ . Physically, this simply says that there is no spin energy for a bond with a hole at one end.

(iii)  $i = \mathbf{R}, j = \mathbf{R} + \hat{\delta}$ . This is the complicated case:

$$M = \frac{1}{2} \sum \langle \{ [c_{\mathbf{R},\sigma}^\dagger c_{\mathbf{R},\sigma'} \mathbf{S}_{\mathbf{R}} \cdot \mathbf{S}_j] + \mathbf{S}_{\mathbf{R}} \cdot \mathbf{S}_j c_{\mathbf{R},\sigma}^\dagger c_{\mathbf{R},\sigma'} \} c_{\mathbf{R}+\hat{\delta},\sigma'}^\dagger c_{\mathbf{R}+\hat{\delta},\sigma''}^\dagger c_{\mathbf{R},\sigma}^\dagger \rangle. \quad (\text{A5})$$

The second term (without the commutator) may be evaluated as in case (i). The commutator is

$$\begin{aligned} [c_{\mathbf{R},\sigma}^\dagger c_{\mathbf{R},\sigma'} \mathbf{S}_{\mathbf{R}} \cdot \mathbf{S}_j] &= \frac{1}{2} \mathbf{S}_j^- [c_{\mathbf{R},\sigma}^\dagger c_{\mathbf{R},\sigma'} c_{\mathbf{R},\uparrow}^\dagger c_{\mathbf{R},\downarrow}] + \frac{1}{2} \mathbf{S}_j^+ [c_{\mathbf{R},\sigma}^\dagger c_{\mathbf{R},\sigma'} c_{\mathbf{R},\downarrow}^\dagger c_{\mathbf{R},\uparrow}] + \mathbf{S}_j^z [c_{\mathbf{R},\sigma}^\dagger c_{\mathbf{R},\sigma'} (c_{\mathbf{R},\uparrow}^\dagger c_{\mathbf{R},\uparrow} - c_{\mathbf{R},\downarrow}^\dagger c_{\mathbf{R},\downarrow})] \\ &= \frac{1}{2} \mathbf{S}_j^- (\delta_{\sigma',\uparrow} c_{\mathbf{R},\sigma}^\dagger c_{\mathbf{R},\sigma'} c_{\mathbf{R},\downarrow} - \delta_{\sigma',\downarrow} c_{\mathbf{R},\sigma}^\dagger c_{\mathbf{R},\sigma'} c_{\mathbf{R},\uparrow}) + \frac{1}{2} \mathbf{S}_j^+ (\delta_{\sigma',\downarrow} c_{\mathbf{R},\sigma}^\dagger c_{\mathbf{R},\sigma'} c_{\mathbf{R},\uparrow} - \delta_{\sigma',\uparrow} c_{\mathbf{R},\sigma}^\dagger c_{\mathbf{R},\sigma'} c_{\mathbf{R},\downarrow}) \\ &\quad + \mathbf{S}_j^z (\delta_{\sigma',\uparrow} c_{\mathbf{R},\sigma}^\dagger c_{\mathbf{R},\sigma'} c_{\mathbf{R},\uparrow} - \delta_{\sigma',\downarrow} c_{\mathbf{R},\sigma}^\dagger c_{\mathbf{R},\sigma'} c_{\mathbf{R},\downarrow} - \delta_{\sigma',\downarrow} c_{\mathbf{R},\sigma}^\dagger c_{\mathbf{R},\sigma'} c_{\mathbf{R},\uparrow} + \delta_{\sigma',\uparrow} c_{\mathbf{R},\sigma}^\dagger c_{\mathbf{R},\sigma'} c_{\mathbf{R},\downarrow}). \end{aligned} \quad (\text{A6})$$

This expression must now be substituted back into  $M$ . The first term involving the operator  $\mathbf{S}_j^-$  is

$$\begin{aligned} M_- &= \frac{1}{2} \sum \langle \frac{1}{2} \mathbf{S}_j^- (\delta_{\sigma',\uparrow} c_{\mathbf{R},\sigma}^\dagger c_{\mathbf{R},\sigma'} c_{\mathbf{R},\downarrow} - \delta_{\sigma',\downarrow} c_{\mathbf{R},\sigma}^\dagger c_{\mathbf{R},\sigma'} c_{\mathbf{R},\uparrow}) c_{\mathbf{R}+\hat{\delta},\sigma'}^\dagger c_{\mathbf{R}+\hat{\delta},\sigma''}^\dagger c_{\mathbf{R},\sigma}^\dagger \rangle \\ &= \frac{1}{4} \sum \langle \mathbf{S}_j^- c_{\mathbf{R}+\hat{\delta},\sigma'}^\dagger c_{\mathbf{R}+\hat{\delta},\sigma''}^\dagger \delta_{\sigma',\uparrow} \delta_{\sigma'',\downarrow} c_{\mathbf{R},\sigma}^\dagger c_{\mathbf{R},\sigma} \rangle - \frac{1}{4} \sum \langle \mathbf{S}_j^- c_{\mathbf{R}+\hat{\delta},\sigma'}^\dagger c_{\mathbf{R}+\hat{\delta},\sigma''}^\dagger \delta_{\sigma',\downarrow} \delta_{\sigma'',\uparrow} c_{\mathbf{R},\sigma}^\dagger c_{\mathbf{R},\sigma} \rangle \\ &= \frac{1}{4} \langle \mathbf{S}_j^- \mathbf{S}_{\mathbf{R}+\hat{\delta}}^+ \rangle - \frac{1}{4} \langle \mathbf{S}_j^- \mathbf{S}_{\mathbf{R}}^+ \rangle. \end{aligned} \quad (\text{A7})$$

The other terms may be evaluated similarly or one may appeal to rotational symmetry to finally obtain

$$M = \frac{1}{2} \langle \mathbf{S}_j \cdot \mathbf{S}_{\mathbf{R}+\hat{\delta}} - \mathbf{S}_j \cdot \mathbf{S}_{\mathbf{R}} \rangle \quad (\text{A8})$$

for case (iii). Finally, combining the three cases, we find

$$M = \frac{1}{2} \sum_{i,j=\mathbf{R},\mathbf{R}+\hat{\delta}} \langle \mathbf{S}_i \cdot \mathbf{S}_j \rangle + \sum_{i=\mathbf{R},j \neq \mathbf{R}+\hat{\delta}} \langle \mathbf{S}_j \cdot \mathbf{S}_{\mathbf{R}+\hat{\delta}} - \mathbf{S}_j \cdot \mathbf{S}_{\mathbf{R}} \rangle + \sum_{i \neq \mathbf{R}+\hat{\delta},j=\mathbf{R}} \langle \mathbf{S}_i \cdot \mathbf{S}_{\mathbf{R}+\hat{\delta}} - \mathbf{S}_i \cdot \mathbf{S}_{\mathbf{R}} \rangle. \quad (\text{A9})$$

<sup>1</sup>J. G. Bednorz and K. A. Müller, Z. Phys. B **64**, 188 (1986); C. W. Chu *et al.*, Phys. Rev. Lett. **58**, 405 (1987).

<sup>2</sup>F. C. Zhang and T. M. Rice, Phys. Rev. **37**, 3759 (1988).

<sup>3</sup>S. Schmitt-Rink, C. Varma, and A. Ruckenstein, Phys. Rev. Lett. **60**, 2793 (1988).

<sup>4</sup>C. Kane, P. Lee, and N. Read, Phys. Rev. B **39**, 6880 (1989).

<sup>5</sup>W. Brinkman and T. Rice, Phys. Rev. B **2**, 1324 (1970).

<sup>6</sup>B. Shraiman and E. Siggia, Phys. Rev. Lett. **61**, 467 (1988).

<sup>7</sup>S. Sachdev, Phys. Rev. B **39**, 12 232 (1989).

<sup>8</sup>S. Trugman, Phys. Rev. B **37**, 1597 (1988).

<sup>9</sup>E. Kaxiras and E. Manousakis, Phys. Rev. B **37**, 656 (1988); **38**, 866 (1988).

<sup>10</sup>E. Dagotto, A. Moreo, and T. Barnes, Phys. Rev. B **40**, 6721 (1989).

<sup>11</sup>J. Bonca, P. Prelovsek, and I. Sega, Phys. Rev. B **39**, 7074 (1989).

<sup>12</sup>J. R. Schrieffer, X. G. Wen, and S. C. Zhang, Phys. Rev. Lett. **60**, 944 (1988); Phys. Rev. B **39**, 11 663 (1989).

<sup>13</sup>T. Barnes, E. Dagotto, A. Moreo, and E. Swanson, Phys. Rev. B **40**, 10977 (1989).

- <sup>14</sup>D. Frenkel, R. Gooding, B. Shraiman, and E. Siggia, *Phys. Rev. B* **41**, 350 (1990).
- <sup>15</sup>J. Bonca and P. Prelovsek (unpublished).
- <sup>16</sup>Y. Nagaoka, *Phys. Rev.* **147**, 392 (1966).
- <sup>17</sup>Y. Fang, A. Ruckenstein, E. Dagotto, and S. Schmitt-Rink, *Phys. Rev. B* **40**, 7406 (1989). See also, B. Doucot and X. G. Wen, *ibid.* **40**, 2719 (1989).
- <sup>18</sup>J. Riera and A. Young, *Phys. Rev. B* **39**, 9697 (1989).
- <sup>19</sup>J. Riera and A. Young, *Phys. Rev. B* **40**, 5285 (1989); A. Barbieri, J. Riera, and A. Young, *Phys. Rev. B* **41** (to be published).
- <sup>20</sup>W. Su, *Phys. Rev. B* **37**, 9904 (1988).
- <sup>21</sup>B. Shraiman and E. Siggia, *Phys. Rev. Lett.* **62**, 1564 (1989).
- <sup>22</sup>Y. Hasegawa and D. Poilblanc, *Phys. Rev. B* **40**, 4035 (1989).
- <sup>23</sup>K.-H. Luk and D. Cox, *Phys. Rev. B* **41**, 4456 (1990).
- <sup>24</sup>T. Barnes *et al.* (unpublished).
- <sup>25</sup>E. Dagotto, A. Moreo, R. Sugar, and D. Toussaint, *Phys. Rev. B* **41**, 811 (1990).
- <sup>26</sup>G. Baskaran, and P. W. Anderson, *Phys. Rev. B* **37**, 580 (1988); I. Affleck, Z. Zou, T. Hsu, and P. W. Anderson, *ibid.* **38**, 745 (1988); E. Dagotto, E. Fradkin, and A. Moreo, *ibid.* **38**, 2926 (1988).
- <sup>27</sup>R. Shankar, *Phys. Rev. Lett.* **63**, 203 (1989).
- <sup>28</sup>J. Marston and I. Affleck, *Phys. Rev. B* **39**, 11 538 (1989).
- <sup>29</sup>E. Dagotto, A. Moreo, R. Joynt, S. Bacci, and E. Gagliano, *Phys. Rev. B* **41**, 2585 (1990).
- <sup>30</sup>P. Horsch, W. Stephan, M. Ziegler, and K. von Szczepanski (unpublished).
- <sup>31</sup>S. A. Trugman, *Phys. Rev. B* **41**, 892 (1990).
- <sup>32</sup>C.-X. Chen, H.-B. Schüttler, and A. Fedro *Phys. Rev. B* **41**, 9495 (1990).
- <sup>33</sup>E. Dagotto and A. Moreo, *Phys. Rev. D* **31**, 865 (1985); E. Gagliano, E. Dagotto, A. Moreo, and F. Alcaraz, *Phys. Rev. B* **34**, 1677 (1986); E. Dagotto and A. Moreo, *ibid.* **38**, 5087 (1988), and references therein.
- <sup>34</sup>H. Mori, *Prog. Theor. Phys.* **33**, 423 (1965); **34**, 399 (1965).
- <sup>35</sup>R. Haydock, V. Heine, and M. Kelly, *J. Phys. C* **5**, 2845 (1972); **8**, 2591 (1975).
- <sup>36</sup>G. Mahan, *Many-Particle Physics* (Plenum, New York, 1981).
- <sup>37</sup>E. Gagliano and C. Balseiro, *Phys. Rev. Lett.* **59**, 2999 (1987). See also, O. Gunnarsson and K. Schönhammer, *Phys. Rev. B* **31**, 4815 (1985); C.-X. Chen and H. Schüttler, *ibid.* **40**, 239 (1989).
- <sup>38</sup>A. Moreo and E. Dagotto, *Phys. Rev. B* **41**, 9488 (1990).
- <sup>39</sup>R. Joynt, *Phys. Rev. B* **37**, 7979 (1988).
- <sup>40</sup>B. Shraiman and E. Siggia, *Phys. Rev. Lett.* **60**, 740 (1988). See also, L. Bulaevskii and D. Khomskii, [*Zh. Eksp. Teor. Fiz.* **52**, 1603 (1967) [*Sov. Phys.—JETP* **25**, 1067 (1967)]; L. Bulaevskii, E. Nagaev, and D. Khomskii, *Zh. Eksp. Teor. Fiz.* **54**, 1562 (1968) [*Sov. Phys.—JETP* **27**, 836 (1968)].
- <sup>41</sup>In Ref. 22 it was independently found that the kinetic energy of the hole has a power-law behavior for small  $J/t$  and it takes the value  $-3.19$  at  $J/t=0$  in very good agreement with our results.
- <sup>42</sup>C.-X. Chen and H. Schüttler, *Phys. Rev. B* **40**, 239 (1989).
- <sup>43</sup>Z. Su, Y. Li, W. Lai, and L. Yu, *Phys. Rev. Lett.* **63**, 319 (1989).
- <sup>44</sup>C. Gros and M. Johnson, *Phys. Rev. B* **40**, 9423 (1989).
- <sup>45</sup>In Ref. 44 the energy at the middle of the dispersive band behaves as  $-3.68 + 2.83J^{0.63}$  [M. Johnson (private communication)].
- <sup>46</sup>D. Reagor, E. Ahrens, S. Cheong, A. Migliori, and Z. Fisk, *Phys. Rev. Lett.* **62**, 2048 (1989); R. Collins, Z. Schlesinger, F. Holtzberg, P. Chaudhari, and C. Feild, *Phys. Rev. B* **39**, 6571 (1989).
- <sup>47</sup>C. Gros, *Phys. Rev. B* **38**, 931 (1988).
- <sup>48</sup>These are obtained from variational calculations on Gutzwiller-type wave functions [R. Joynt (unpublished)].
- <sup>49</sup>N. Bulut, D. Hone, E. Loh, and D. Scalapino, *Phys. Rev. Lett.* **62**, 2192 (1989).
- <sup>50</sup>B. Friedman, X. Chen, and W. Su, *Phys. Rev. B* **40**, 4431 (1989).
- <sup>51</sup>S. White, D. Scalapino, R. Sugar, and N. Bickers, *Phys. Rev. Lett.* **63**, 1523 (1989).